ACS Infectious Diseases

pubs.acs.org/journal/aidcbc

Article

Small-Molecular Adjuvants with Weak Membrane Perturbation Potentiate Antibiotics against Gram-Negative Superbugs

Geetika Dhanda, Riya Mukherjee, Debajyoti Basak, and Jayanta Haldar*

Cite This: *ACS Infect. Dis.* 2022, 8, 1086−1097

Read Online

ACCESS | Metrics & More | Article Recommendations | Supporting Information

ABSTRACT: Combination therapy with membrane-targeting compounds is at the forefront because the bacterial membrane is an attractive target considering its role in various multidrug-resistant elements. However, this strategy is crippled by the toxicity associated with these agents. The structural requirements for optimum membrane perturbation and minimum toxicity have not been explored for membrane-targeting antibiotic potentiators or adjuvants. Here, we report the structural influence of different chemical moieties on membrane perturbation, activity, toxicity, and potentiating ability in norspermidine derivatives. It has been shown in this report that weak membrane perturbation, achieved by the incorporation of cyclic hydrophobic moieties, is an effective strategy to design antibiotic adjuvants with negligible *in vitro* toxicity and activity but good potentiating ability. Aryl or adamantane functionalized derivatives were found to be better resorts as opposed to the acyclic analogues, exhibiting as high as 4096-fold potentiation of multiple classes of antibiotics toward critical Gram-negative superbugs. The mechanism of potentiation was nonspecific, consisting of weak outer-membrane permeabilization, membrane depolarization, and efflux inhibition. This unique concept of "weakly perturbing the membrane" by incorporating cyclic hydrophobic moieties in a chemical design with free amine groups serves as a breakthrough for nontoxic membrane-perturbing adjuvants and has the potential to revitalize the effect of obsolete antibiotics to treat complicated Gram-negative bacterial infections.

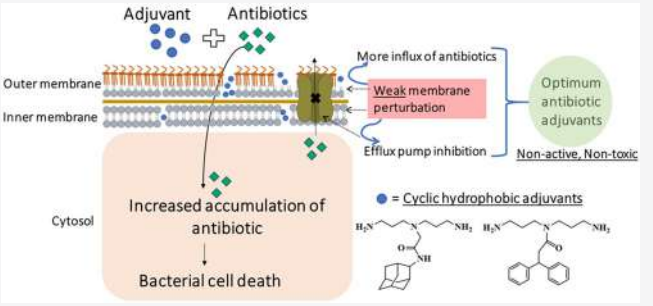

KEYWORDS: *adjuvants, antibiotics, antimicrobial resistance, Gram-negative bacteria, membrane perturbation*

Antimicrobial resistance (AMR) is one of the world's most urgent public health problems, annually claiming around 700,000 lives on the global front.[1] The World Health Organization (WHO) has enlisted Gram-negative bacteria *Acinetobacter baumannii*, *Pseudomonas aeruginosa*, and multidrug-resistant (MDR) *Enterobacteriaceae* spp. as the most critical infection-causing pathogens.[2] Bacterial coinfections and secondary infections have been identified with other infections like COVID-19 as well.[3] The sluggish development of new antibiotics and the increasing resistance to existing drugs call for immediate interventions. The high-resistance phenotype seen in Gram-negative bacteria is due to their outer-membrane barrier composed of lipopolysaccharide, the expression of MDR efflux pumps, most of which are mediated by the proton gradient, and the presence of enzymes like β-lactamases.[4,5] Out of these three mechanisms, the first two are ubiquitously found in different Gram-negative superbugs due to which a vast number of classes of antibiotics are rendered ineffective. Outer-membrane impermeability is an intrinsic resistance element, which depends on the integrity of the bacterial membrane. The function of most efflux pumps (other than the adenosine 5′-triphosphate (ATP) binding cassette family) depends on the bacterial membrane potential.[6] Indirectly targeting the above-mentioned common resistance elements through membrane-targeting strategies can revitalize the efficacy of a huge chunk of the existing antibiotic arsenal.[7−10]

In addition to assessing the antimicrobial activity of membrane-active compounds and synthetic mimics of antimicrobial peptides (AMPs),[11] they have also been tested in combination with antibiotics.[12−17] The bacterial membrane is an alluring target because of its role in maintaining cellular homeostasis, proton-motive force, energy transduction, active transport of nutrients and waste, and respiration.[10] However, high membrane-activity often results in associated toxicity. Also, due to the emergence of MDR bacterial strains, there is a pertinent need to develop more nonantibiotic components (adjuvants) in synergistic combinations, which directly or indirectly target resistance pathways rather than exert any self-activity.[8] For membrane-perturbing compounds, the relation of extent of membrane perturbation has not been well studied with potentiating capacity, activity, and toxicity. The optimum

Received: February 13, 2022
Published: April 11, 2022

Scheme 1. Synthesis of Small-Molecular Adjuvants

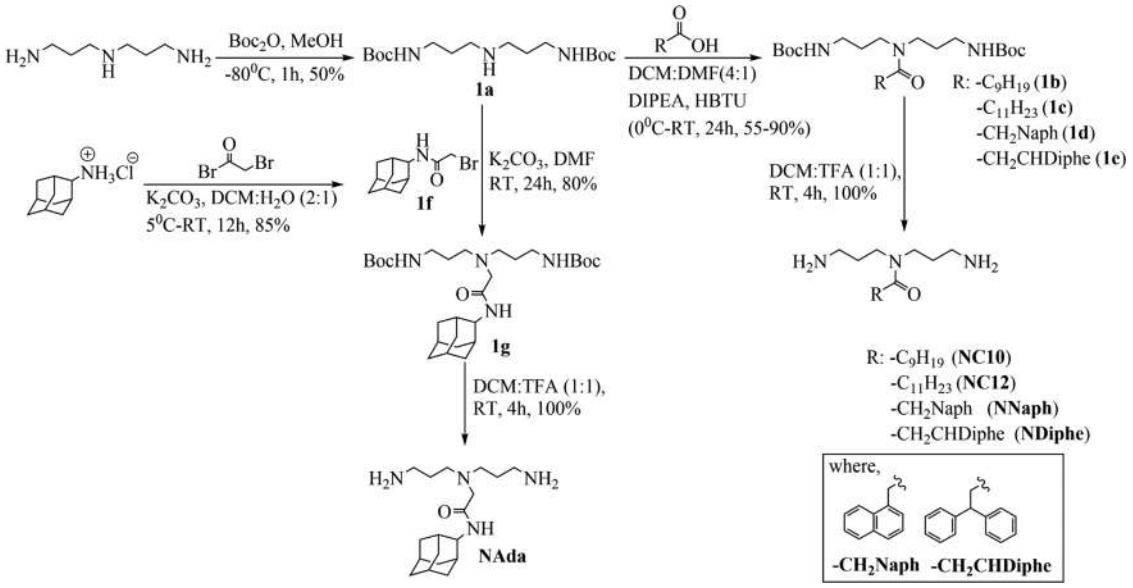

extent of membrane perturbation to design membrane-perturbing antibiotic adjuvants is highly elusive. The structural influence of different chemical moieties on membrane perturbation and their subsequent role in designing nontoxic adjuvants has also not been stressed upon. There is a need to understand these effects so that the design of molecules can be modulated to result in desired properties: nonactivity, nontoxicity, and high potentiation.

Here, we report a thorough comparison of membrane-perturbing properties of norspermidine derivatives with acyclic aliphatic hydrophobicity (decyl and dodecyl derivatives), cyclic hydrophobicity (naphthyl, diphenyl, and adamantane bearing derivatives), and a strong membrane-perturbing surfactant, cetyl trimethylammonium bromide (CTAB). Norspermidine was chosen as the model compound because of its primary amines, which at physiological pH would interact with the negatively charged bacterial membrane. Different types of hydrophobic groups were appended to its secondary amine to ascertain the optimum type of hydrophobicity to ensure less toxicity and high potentiation ability. The membrane perturbation is correlated with activity, toxicity at the mitochondrial level, and potentiation ability. The mechanism of potentiation was also determined by assessing outer-membrane permeabilization and membrane depolarization and other related properties like inhibition of antibiotic efflux, accumulation of antibiotics, and leakage of dye in liposomes. The generic and broad-spectrum nature of the best adjuvant was determined by assessing the potentiation of multiple antibiotics against clinical isolates of different Gram-negative bacteria.

RESULTS AND DISCUSSION

Design and Synthesis. Lipophilic analogues of a symmetric triamine, norspermidine, with varying hydrophobic moieties were synthesized (Scheme 1). Norspermidine was chosen as its primary amines will be positively charged at the physiological pH, which will help in interaction with the negatively charged bacterial membrane. Moreover, it is an inexpensive compound that allows facile functionalization. Five derivatives with different types of hydrophobicity were synthesized. Acyclic aliphatic groups with lipophilic chains greater than 12 carbons were not synthesized as higher-chain aliphatic analogues were previously shown to be active and toxic.[18]

Briefly, the primary amines of norspermidine were first protected by the tertiary butoxy carbonyl (Boc) group to yield **1a**. Then, the secondary amine was conjugated with different types of hydrophobic moieties *via* *O*-(1*H*-benzotriazol-1-yl)-*N*,*N*,*N*′,*N*′-tetramethyluronium hexafluorophosphate (HBTU) coupling or a nucleophilic substitution reaction. The hydrophobic moieties were acyclic; decyl (**NC10**), dodecyl (**NC12**), and cyclic; naphthyl (**NNaph**), diphenyl (**NDiphe**), and adamantane (**NAda**). The detailed characterization is given in the Supporting Information.

Assessment of Membrane-Perturbation Properties in Live Bacteria. Due to the presence of primary amines and hydrophobic groups in the molecular design, the derivatives are expected to interact with negatively charged phospholipids of the bacterial

membrane. To confirm this hypothesis, the compounds were tested for membrane perturbation by assessing outer-membrane permeabilization and membrane depolarization through fluorescence assays[19] against *A. baumannii* and *P. aeruginosa*, the two topmost critical bacterial pathogens. The bacterial proton-motive force (PMF) is composed of the transmembrane electrical potential ($\Delta\Psi$) and the transmembrane chemical gradient (ΔpH).[20] The cytoplasmic membrane depolarization was evaluated for the bacteria using $DiSC_3(5)$ (3,3′-dipropylthiadicarbocyanine iodide). $DiSC_3(5)$ accumulates in the cytoplasmic membrane of the energized cells due to which its fluorescence is quenched.[18] If the membrane is perturbed, the dye is released into the solution, showing an increase in fluorescence. Similarly, *N*-phenyl-1-naphthylamine (NPN) was used to determine outer-membrane permeabilization in bacterial cells. An intact outer membrane excludes substances such as NPN, but a perturbed outer membrane results in the entry of NPN molecules into the phospholipid layer, thereby showing an increase in fluorescence.[21] The normalized fluorescence intensity at the end of ~40 min was plotted for both of these assays in Figure

https://doi.org/10.1021/acsinfecdis.2c00092
ACS Infect. Dis. 2022, 8, 1086−1097

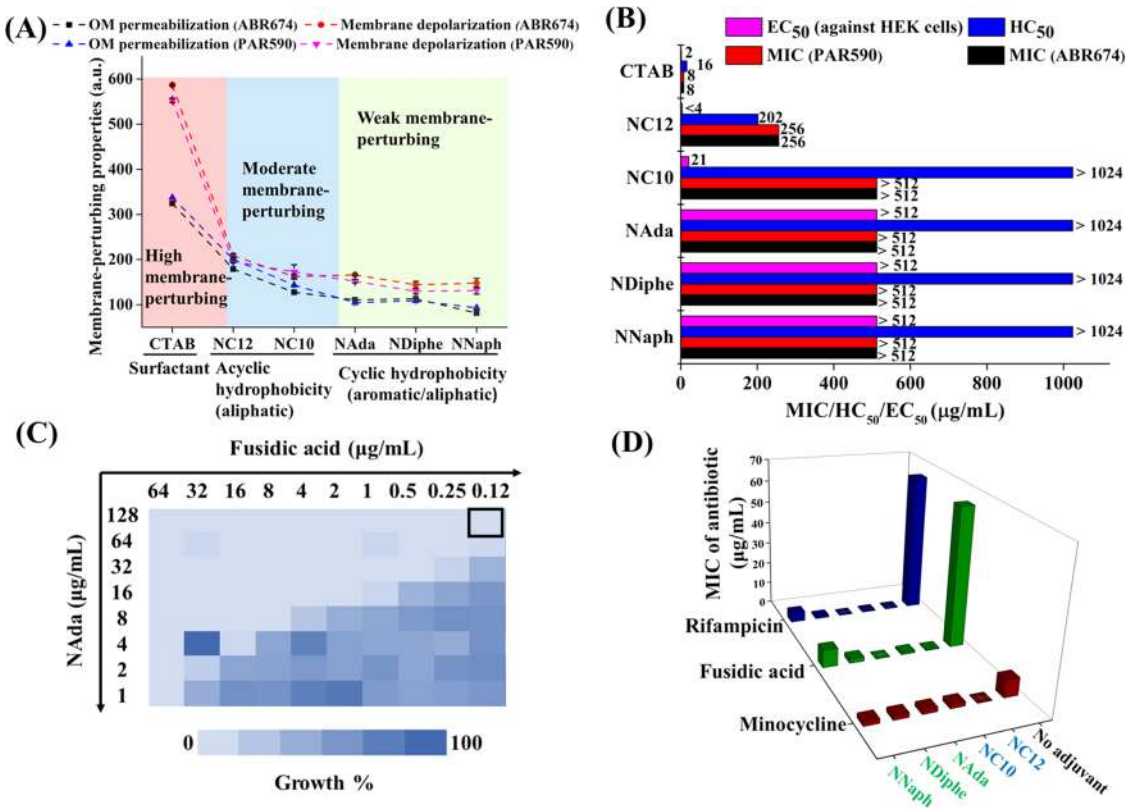

Figure 1. Classification of compounds based on biophysical and microbiological properties (A) characterization based on membrane-perturbing properties (outer-membrane permeabilization and membrane depolarization). Normalized fluorescence intensity was plotted to demarcate membrane-perturbing properties (*y*-axis). (B) Activity and toxicity of compounds. (C) Chequerboard assay of fusidic acid with **NAda** against *A. baumannii* R674. (D) Potentiating activity with minocycline, fusidic acid, and rifampicin against *A. baumannii* R674. Concentration of adjuvants (μg/mL) used for minocycline, fusidic acid, and rifampicin: **NC12:** 128, 64, 16; **NC10**: 32, 64, 64; **NAda**: 128, 128, 128; **NDiphe:** 16, 128, 128; **NNaph**: 64, 128, 128. MIC, minimum inhibitory concentration; HEK cells, human embryonic kidney 293 cells; EC_{50}, effective concentration to kill 50% cells; HC_{50}, concentration to lyse 50% of human red blood cells (hRBCs).

1A upon treatment with different compounds, which demarcated the extent of membrane perturbation properties (*y*-axis of Figure 1A). CTAB, a common surfactant with a positive charge and long acyclic hydrophobicity, was taken as a control. All compounds exhibited some level of outer-membrane permeabilization and membrane depolarization, indicating their interaction with the bacterial membrane. However, the extent of perturbation was different for all of the compounds, and this was highly dependent on the type of hydrophobic moiety in the chemical design. The compounds could roughly be grouped into three categories according to the extent of membrane perturbation. CTAB (surfactant) constituted the high membrane-perturbing region; **NC12** and **NC10** (acyclic hydrophobic) exhibited slightly more fluorescence intensity as compared to the cyclic hydrophobic compounds; **NAda**, **NDiphe**, and **NNaph**. Through this, we conjecture that the acyclic hydrophobic compounds are moderately membrane-perturbing as compared to the weak membrane-perturbing cyclic hydrophobic compounds (Figures 1A and S9). To confirm this conjecture, antibacterial activity, toxicity, potentiation ability, and dye leakage studies in liposome mimics were performed in subsequent studies.

***In Vitro* Antibacterial Activity, Toxicity, and Potentiation Ability.** The absence of any activity reduces the propensity of resistance development to the adjuvant, and the nontoxic nature is essential for translation of adjuvants into clinics.[12] The "cyclic hydrophobic" adjuvants; **NAda**, **NDiphe**, and **NNaph** exhibited no activity with MIC > 512 μg/mL against *A. baumannii* and *P. aeruginosa* (Figure 1B). These adjuvants also exhibited no toxicity (EC_{50} > 512 μg/mL and HC_{50} > 1024 μg/mL) against mammalian cells.

Among the "acyclic hydrophobic" adjuvants, **NC10** was nonactive with an MIC of >512 μg/mL against both bacteria and nontoxic toward human erythrocytes (HC_{50} > 1024 μg/mL). However, **NC10** was toxic toward HEK cells with an EC_{50} of 21 μg/mL. **NC12** was slightly more active (MIC = 256 μg/mL) but highly toxic (HC_{50} = 202 μg/mL, EC_{50} < 4 μg/mL). The high membrane-perturbing agent, CTAB, showed high activity (MIC = 8 μg/mL) and high toxicity (HC_{50} = 16 μg/mL, EC_{50} = 2 μg/mL). Then, the capacity of the synthesized compounds as antibiotic adjuvants was determined against *A. baumannii* R674 by performing chequerboard assays (Figures 1C and S1−S3) of these compounds with three antibiotics from different classes: minocycline, fusidic acid, and rifampicin (Figure 1D). Hydrophobic antibiotics like fusidic acid and rifampicin are used for Gram-positive infections and tuberculosis, respectively. Gram-negative pathogens are inherently resistant to these antibiotics because of the impermeability posed by the outer lipopolysaccharide membrane.[22] Minocycline is an example of tetracycline antibiotics that have become obsolete against resistant Gram-negative bacteria due to efflux pumps like TetA and AcrAB-TolC as one of the reasons for resistance.[23,24] All adjuvants showed potentiation of the antibiotics, with **NC12** and **NAda** showing

https://doi.org/10.1021/acsinfecdis.2c00092
ACS Infect. Dis. 2022, 8, 1086−1097

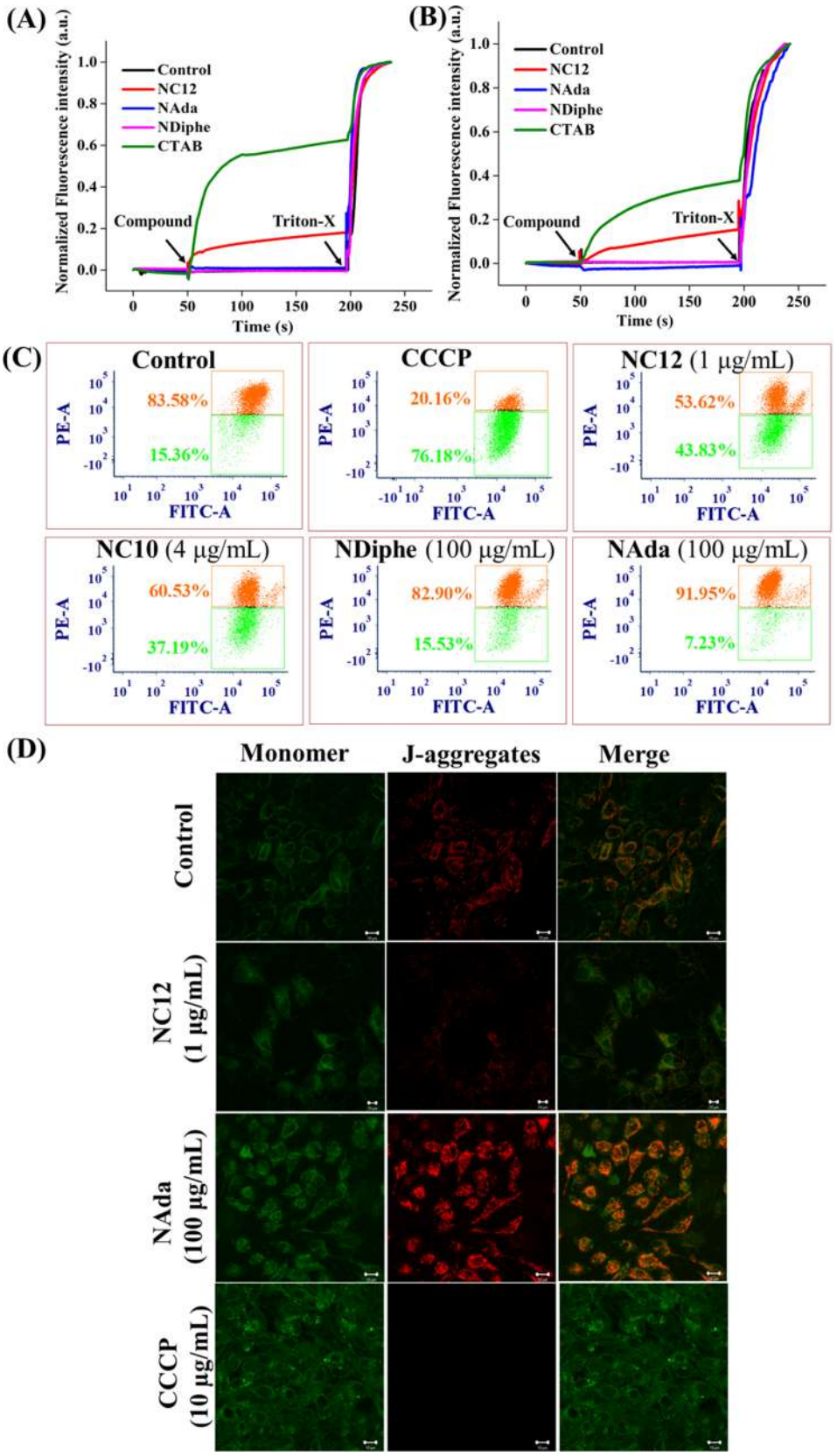

Figure 2. Leakage of carboxyfluorescein in (A) bacterial membrane mimic and (B) mammalian membrane mimic. (C) Analysis of mitochondrial membrane potential of HEK 293 cells by studying the formation of *J*-aggregates through flow cytometry. (D) Assessment of formation of *J*-aggregates through confocal microscopy (CLSM). Scale bar in CLSM images is 10 μm. Control refers to vehicle control.

the best results. **NC12** showed 32−128-fold reduction in MIC of antibiotics (0.25−0.5 μg/mL) at a concentration of 16−128 μg/mL, and **NAda** exhibited 4−512-fold potentiation ($MIC_{antibiotic}$ = 0.125−2 μg/mL) at a concentration of 128

https://doi.org/10.1021/acsinfecdis.2c00092
ACS Infect. Dis. 2022, 8, 1086−1097

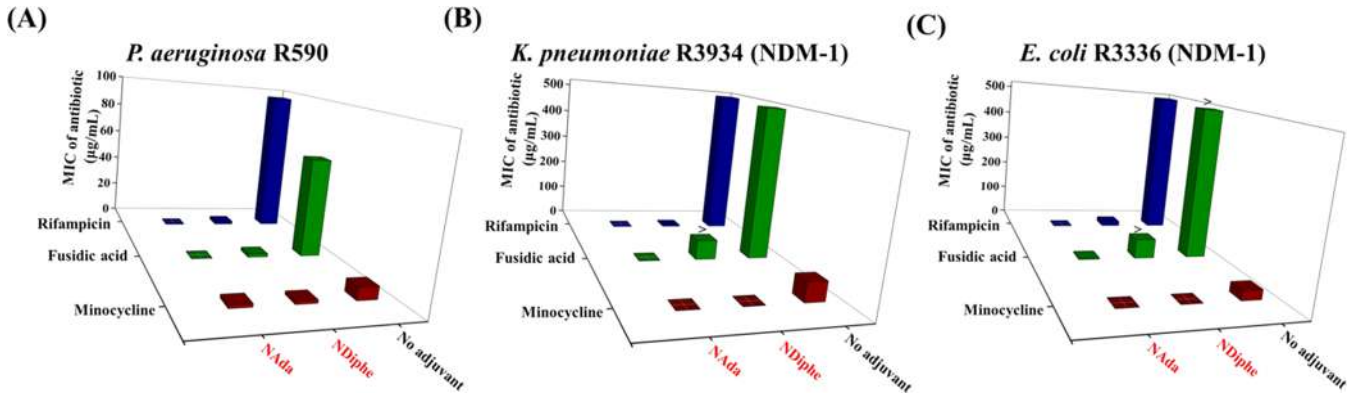

Figure 3. Potentiation capacities of **NAda** and **NDiphe** against multidrug-resistant Gram-negative superbugs, including NDM-1 bacteria. The MIC of antibiotics in the presence of **NAda** and **NDiphe** (128 μg/mL) against (A) *P. aeruginosa* R590, (B) *K. pneumoniae* R3934, and (C) *E. coli* R3336.

μg/mL. **NC10** was the next good adjuvant showing 4−128-fold improvement in MIC values at a concentration of 32−64 μg/mL. **NDiphe** and **NNaph** exhibited 4−64-fold potentiation at a concentration of 16−128 μg/mL and 4−14-fold potentiation at a concentration of 64−128 μg/mL, respectively. The exact concentration of adjuvants used for each antibiotic is mentioned in Figure 1 caption and Table S1. To summarize, all of the adjuvants depicted some level of potentiation by reducing the MICs of obsolete antibiotics to a clinically acceptable range (<4 μg/mL) in most of the cases. A strong structural influence of hydrophobicity was observed on the properties of compounds. Compounds with cyclic hydrophobicity (aliphatic and aromatic) showed weak membrane perturbation but did not show any activity and toxicity while potentiating the antibiotics at nontoxic concentrations (16−128 μg/mL). Compounds with "acyclic hydrophobicity" showed moderate membrane perturbation, less activity, higher toxicity, and only potentiated the antibiotics at toxic concentrations (16−128 μg/mL). The surfactant control CTAB showed high membrane perturbation, good activity, and high toxicity. Thus, it was concluded that weak membrane perturbation was enough for compounds to have the potentiation effects on antibiotics without showing any toxicity. The distinction between weak and moderate membrane-perturbing compounds was further validated through subsequent studies.

Leakage of Carboxyfluorescein Dye through Liposome Mimics of Membranes. To validate our conjecture that cyclic hydrophobic compounds are weak membrane-perturbing and acyclic hydrophobic compounds are moderately membrane-perturbing, further studies on liposome mimics of bacteria and mammalian cells were performed. A bacterial membrane mimic consisting of dipalmitoylphosphatidylglycerol (DPPG) and dipalmitoylphosphatidylethanolamine (DPPE) (DPPG/DPPE = 88:12) and a mammalian membrane mimic consisting of dipalmitoylphosphatidylcholine (DPPC) encapsulated with a concentration-dependent fluorescent dye, carboxyfluorescein, were treated with adjuvants from each class at 320 μg/mL, and the dye leakage was studied. At 200 s, a nonionic surfactant, Triton-X, was added to cleave the vesicle and release the dye into the solution, which resulted in the maximum fluorescence value. CTAB and **NC12** were able to cause dye leakage due to their excessive and moderate membrane perturbation, respectively (Figure 2A,B). **NAda** and **NDiphe** did not exhibit any dye leakage in either of the membranes. No leakage of carboxyfluorescein by cyclic hydrophobic compounds **NAda** and **NDiphe** from bacterial and mammalian membrane mimics further proves their nontoxic and weak membrane-perturbing nature. This correlates with biophysical studies in live bacteria and further confirms the weak membrane perturbation caused by **NAda** and **NDiphe**, which makes them nontoxic toward mammalian cells and nonactive toward bacteria. It also validates that acyclic hydrophobic compounds like **NC12** were moderate membrane-perturbing in nature, which makes them different from the weak membrane-perturbing cyclic hydrophobic compounds.

Assessment of Toxicity by Studying Mitochondrial Membrane Depolarization. Detailed toxicity was assessed by studying the effect of the compounds on mitochondrial membrane depolarization through tetraethylbenzimidazolylcarbocyanine iodide (JC-1) dye in HEK 293 cells (Figures 2C,D and S4). Since mitochondria is known to be high in negatively charged lipids like phosphatidylglycerol and cardiolipin and has a $\Delta\Psi$, highly negative on the inside, it is comparable to the bacterial membrane.[25,26] Also, mitochondrial membrane depolarization signifies earlier stages of mitophagy, which should be avoided in healthy cells. Thus, it is important to study the effect of compounds on mitochondrial membrane. JC-1 dye accumulates in the mitochondria and forms *J*-aggregates at a negative mitochondrial membrane potential. If the membrane potential depolarizes, JC-1 accumulation is not observed and there is green fluorescence associated with the monomer. Carbonyl cyanide *m*-chlorophenyl hydrazone (CCCP) was used as the positive control, which is known to show depolarization in mitochondria. **NC12** and **NC10**, the acyclic aliphatic compounds, showed 44 and 37% cells with depolarized mitochondrial membranes, as shown by only green fluorescence. **NAda** and **NDiphe** showed flow cytometry distribution like the control, which signifies healthy cells where no treatment was given, with 7.2 and 15.5% cells having depolarized mitochondrial membranes. The control showed 15.4% similar cells. CTAB and CCCP exhibited high levels of mitochondrial membrane depolarization (Figures 2C and S4). The same observation was also confirmed by confocal microscopy (Figures 2D and S4). Assessment of mitochondrial membrane depolarization indicated early signs of mitophagy in cells treated with strong and moderate membrane-perturbing compounds, even at nontoxic concentrations. These experiments further emphasize the importance of weak membrane perturbation through cyclic hydrophobic moieties in designing nonactive and nontoxic adjuvants.

https://doi.org/10.1021/acsinfecdis.2c00092
ACS Infect. Dis. 2022, 8, 1086−1097

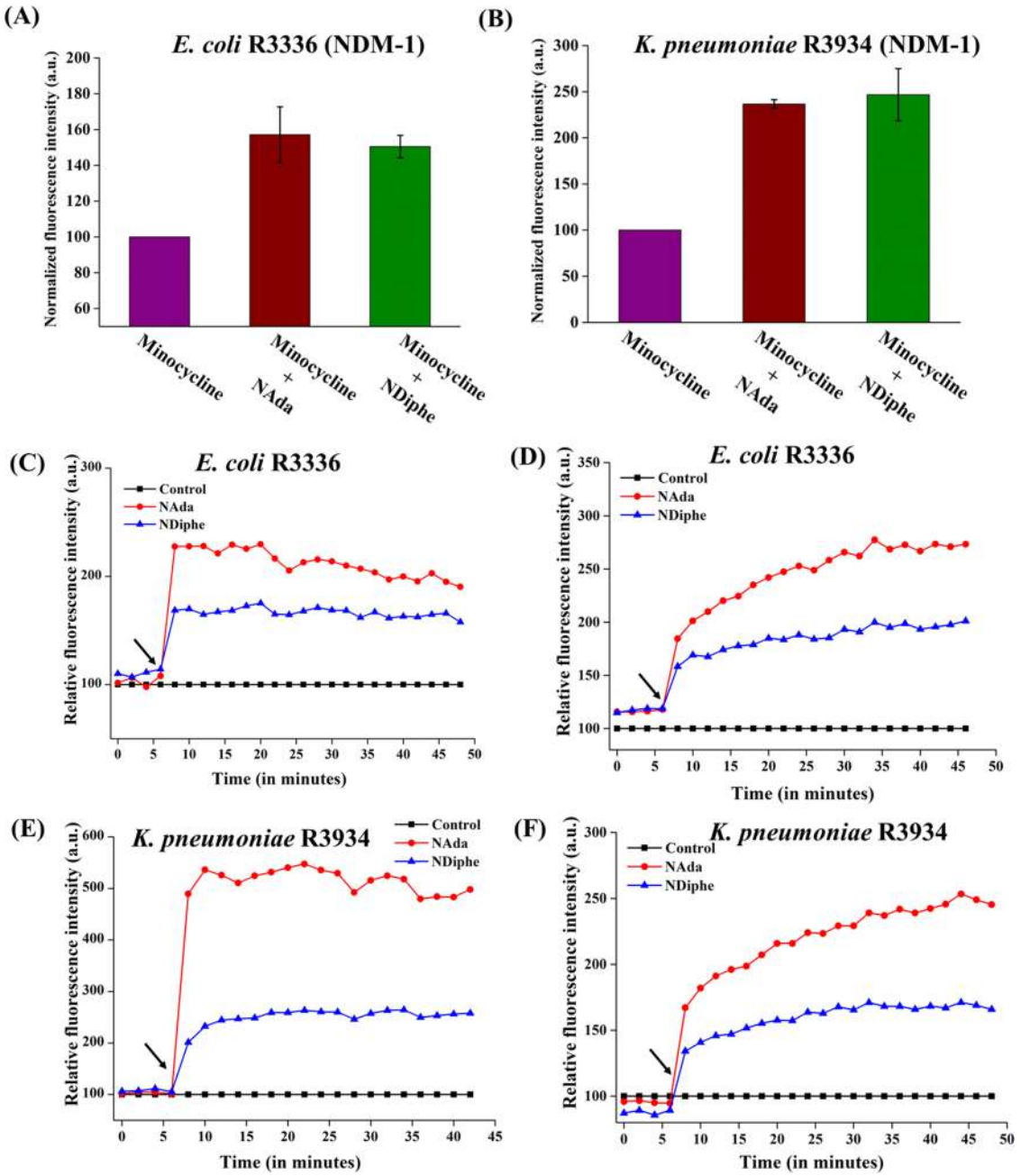

Figure 4. Mechanism of potentiation by **NAda** and **NDiphe**. Accumulation of minocycline (128 μg/mL) in the presence of **NAda** (100 μg/mL) and **NDiphe** (100 μg/mL) after 30 min in (A) *E. coli* R3336 and (B) *K. pneumoniae* R3934. (C) Outer-membrane permeabilization in *E. coli* R3336, (D) membrane depolarization in *E. coli* R3336, (E) outer-membrane permeabilization in *K. pneumoniae* R3934, and (F) membrane depolarization in *K. pneumoniae* R3934 in the presence of **NAda** (100 μg/mL) and **NDiphe** (100 μg/mL). Arrow indicates the time of compound addition.

Broad-Spectrum Potentiation Ability of Adjuvants. After optimizing **NAda** and **NDiphe** as the best adjuvants and studying their biophysical and microbiological properties, the potentiation of **NAda** and **NDiphe** was assessed against MDR isolates of other critical Gram-negative bacteria, including New Delhi metallo-β-lactamase-1 (NDM-1) producing strains to determine their spectrum of activity. The MIC of antibiotics in the presence of 128 μg/mL adjuvants was plotted (Figure 3). From this, the potentiation factors (Figure S5) were inferred. **NAda** exhibited 8−768-fold potentiation (MIC of antibiotics was 0.125−2 μg/mL in the presence of **NAda**) against *P. aeruginosa* (Figure 3A). **NAda** reduced the MIC of antibiotics to 0.25−1 μg/mL (128−2048-fold) against *Klebsiella pneumoniae* and to 0.125−4 μg/mL (32−4096-fold) against *Escherichia coli* (Figure 3B,C). For **NDiphe**, the potentiation factors were 4−48 (MIC of antibiotics = 2 μg/mL) against *P. aeruginosa* (Figure 3A). Against NewDelhi metallo-β-lactamase-1 (NDM-1) producing bacteria *E. coli* R3336 and *K. pneumoniae* R3934, less potentiation was observed with fusidic acid in the presence of **NDiphe** as the MIC was >64 μg/mL (Figure 3B,C). This needs to be investigated further. Against *K. pneumoniae*, **NDiphe** reduced the MIC of rifampicin to 4 μg/mL (128-fold) and of minocycline to 1 μg/mL (64-fold) (Figure 3B). Against *E. coli*, **NDiphe** reduced the MIC of

https://doi.org/10.1021/acsinfecdis.2c00092
ACS Infect. Dis. 2022, 8, 1086−1097

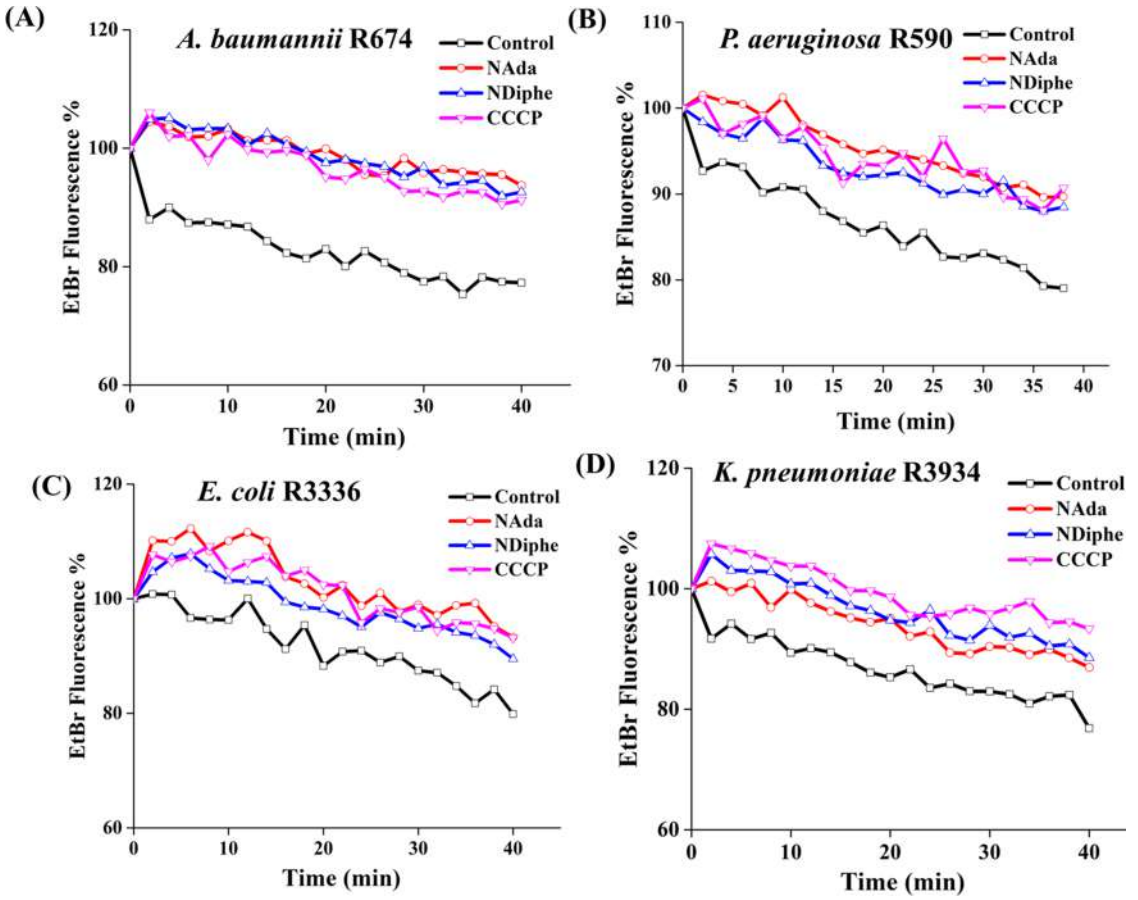

Figure 5. Mechanism of potentiation by **NAda** and **NDiphe**. Inhibition of EtBr efflux by **NAda** (100 μg/mL), **NDiphe** (100 μg/mL), or CCCP (20 μg/mL) in (A) *A. baumannii* R674, (B) *P. aeruginosa* R590, (C) *E. coli* R3336, and (D) *K. pneumoniae* R3934.

rifampicin to 16 μg/mL (32-fold) and of minocycline to 1 μg/mL (32-fold; Figure 3C). These studies show that **NAda** showed broad-spectrum potentiation of minocycline, rifampicin, and fusidic acid against multiple strains of Gram-negative superbugs. Various trends of the potentiation factors for **NAda** and **NDiphe** with different antibiotics and concentrations are depicted in the SI (Figures S5−S7).

Accumulation of Antibiotics Inside the Bacteria and Membrane-Perturbing Properties. To support the better accumulation of antibiotics inside bacteria due to outer-membrane permeabilization and membrane depolarization of the adjuvants, the overall uptake of fluorescent minocycline (128 μg/mL) was studied in the presence of **NAda** and **NDiphe** in NDM-1-producing bacteria *E. coli* R3336 and *K. pneumoniae* R3934 (Figures 4A,B and S8A,B). The normalized fluorescence of minocycline was higher in the presence of adjuvants as compared to the control at the end of 30 min. This signifies increased accumulation of the antibiotic in the presence of an adjuvant. Accumulation studies of minocycline showed increased intracellular concentration of the antibiotic in the bacteria. Outer-membrane permeabilization and membrane depolarization of *E. coli* and *K. pneumoniae* in the presence of **NAda** and **NDiphe** were also confirmed (Figure 4C−F) using fluorimetry assays described in the previous section. Both the compounds exhibited outer-membrane permeabilization and cytoplasmic membrane depolarization against NDM-1-producing strains of bacteria. These are the tools with the help of which the adjuvant helps in better accumulation of the antibiotic inside the bacterial cell. The increased accumulation of the antibiotic might pertain to more uptake due to outer-membrane permeabilization, more ΔpH-dependent uptake because of membrane depolarization,[27] and less efflux due to impairment of the efflux machinery, as a result of membrane depolarization. We believe that as our adjuvants decreased the $\Delta\Psi$ component of the proton-motive force, it might have to be compensated for by an increase in the ΔpH component of PMF, which would drive the uptake of minocycline. All of the above-mentioned factors, combined, resulted in more accumulation of the antibiotic inside bacterial cells. The inhibition of efflux pumps was checked further to confirm the effect of membrane depolarization on the efflux machinery in bacteria.

Impairment of Efflux Machinery. Various efflux pumps in bacteria that are responsible for extrusion of antibiotics are highly dependent on the membrane potential and proton-motive force.[28] In Gram-negative bacteria, different types of efflux pumps are present like the ATP-binding cassette (ABC), major facilitator superfamily (MFS), multidrug and toxin extrusion (MATE), small multidrug resistance (SMR), and resistance-nodulation-cell division (RND) families.[28] Except for the ABC family, the functioning of all other efflux pumps is dependent on the proton gradient across the bacterial cell. Considering that the adjuvants depolarized the membrane in bacteria, their effect on the efflux machinery was tested. The impairment of efflux machinery was confirmed for **NAda** and **NDiphe** by reduction in the efflux of ethidium bromide (EtBr), a common substrate for most MDR efflux pumps[29] (Figure 5). In *A. baumannii*, about 20% reduction in EtBr efflux

https://doi.org/10.1021/acsinfecdis.2c00092
ACS Infect. Dis. 2022, 8, 1086−1097

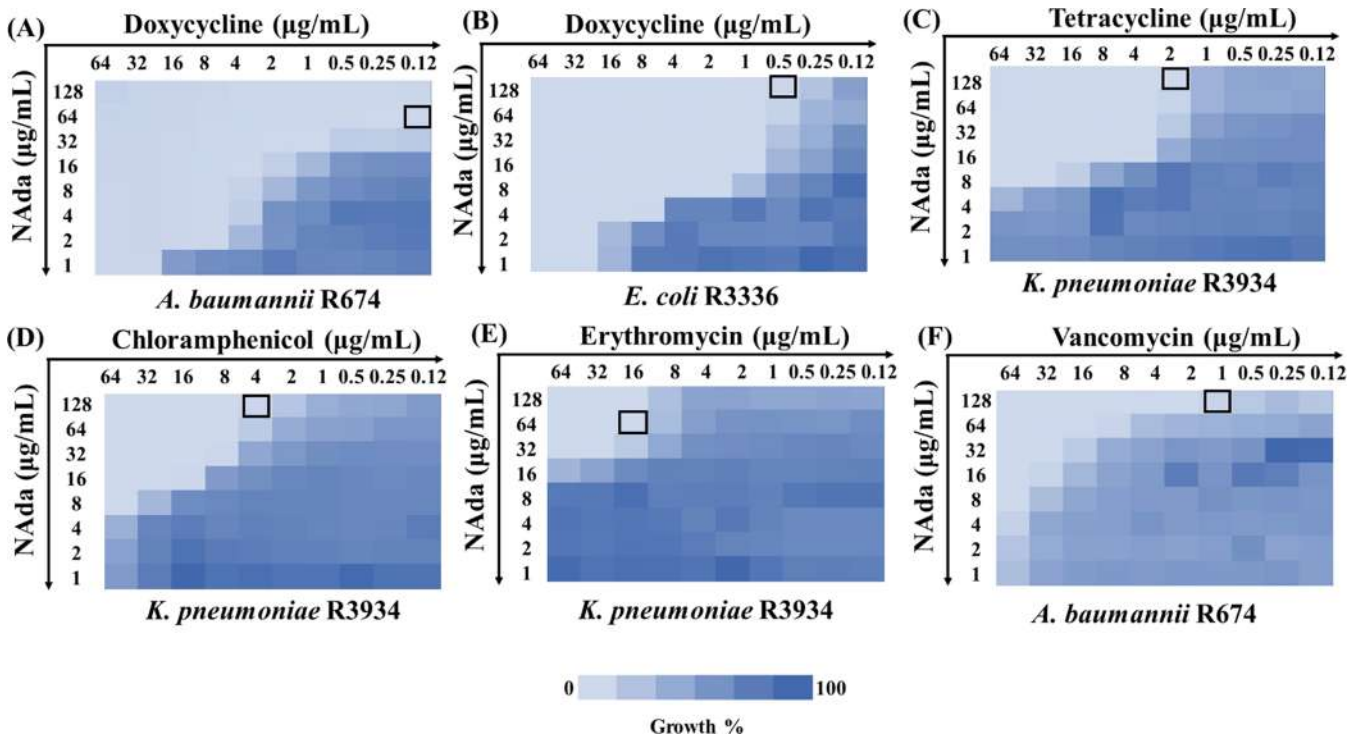

Figure 6. Potentiation of different classes of antibiotics by **NAda** against MDR bacteria. Chequerboard assay of (A) doxycycline and **NAda** against *A. baumannii* R674; (B) doxycycline and **NAda** against *E. coli* R3336; (C) tetracycline and **NAda** against *K. pneumoniae* R3934; (D) chloramphenicol and **NAda** against *K. pneumoniae* R3934; (E) erythromycin and **NAda** against *K. pneumoniae* R3934; and (F) vancomycin and **NAda** against *A. baumannii* R674.

was observed in the first 40 min as compared to the untreated control (Figure 5A). For *P. aeruginosa*, *E. coli*, and *K. pneumoniae*, about 10% reduction in efflux was observed in the first 40 min (Figure 5B−D). The reduction in efflux was comparable to CCCP, which is a known efflux pump inhibitor.[30] Reduced efflux of EtBr in the presence of **NAda** and **NDiphe** indicates that membrane depolarization might lead to ion disbalance, which indirectly affects efflux pumps and slows down the efflux of substrates like antibiotics and EtBr. This proves that weak membrane perturbation counters resistance elements by slight outer-membrane permeabilization, slight membrane depolarization, inhibition of efflux, and the resultant increased accumulation of antibiotics in the bacterial cell.

Ubiquitous Potentiation of Multiple Antibiotics. To further the ubiquitous potentiation by the best adjuvant, chequerboard assays of **NAda** were performed with antibiotics of different classes like doxycycline, tetracycline, erythromycin, vancomycin, and chloramphenicol. Potentiation (4-fold to >512-fold) was observed with these antibiotics against different strains of bacteria (Figures 6A−F and S10, Table S3). Potentiation was observed with the maximum number of strains with all antibiotics. A few representative chequerboards are shown in Figure 6A−F, and the rest of the chequerboards are shown in Figure S10, with data in Table S3.

Tetracycline was potentiated by 8−256-fold against all four strains of MDR bacteria in the presence of **NAda**. Similarly, **NAda** showed 8−512-fold potentiation of another tetracycline antibiotic, doxycycline, against all tested bacteria. Potentiation of erythromycin of 32-fold was observed against the tested strains except for *E. coli* R3336. Potentiation of vancomycin of 4−64-fold was observed against the tested strains except for the NDM-1-producing bacteria. Potentiation of chloramphenicol of 4−64-fold was observed against the tested bacteria except for *E. coli* R3336. Less or no potentiation of erythromycin, vancomycin, and chloramphenicol against either one or both of the NDM-1-producing bacteria is probably because of additional resistance elements present in these bacteria toward the mentioned antibiotics. This is possible because the plasmids encoding for NDM-1 often carry genes, which confer resistance to other antibiotics like aminoglycosides, quinolones, macrolides, and chloramphenicol.[31] However, this needs to be investigated further. As erythromycin and tetracycline antibiotics have become obsolete due to the efflux pumps present in MDR bacteria,[23,32] membrane depolarization and efflux pump inhibition are the expected mechanisms for potentiation of antibiotics from the tetracycline class and erythromycin. Outer-membrane permeabilization might also help in more uptake of these antibiotics and result in better activity. For rifampicin, fusidic acid, vancomycin, and chloramphenicol, outer-membrane permeabilization might just be enough as the mechanism of potentiation. These antibiotics are usually inactive against Gram-negative bacteria because of the outer-membrane barrier.[4]

■ CONCLUSIONS

To solve the ever-increasing problem of AMR, innovative strategies and nontraditional therapeutic approaches are required. One such approach is rehabilitation of obsolete antibiotics by the use of antibiotic adjuvants. Combining this approach with an attractive target, the bacterial membrane, we have designed generic and nontoxic antibiotic adjuvants. Structure−activity relationship revealed that compounds with cyclic hydrophobic groups appended to the secondary amine

https://doi.org/10.1021/acsinfecdis.2c00092
ACS Infect. Dis. 2022, 8, 1086−1097

of norspermidine caused weak membrane perturbation, no *in vitro* activity until the tested concentration (*i.e.*, 512 μg/mL), negligible *in vitro* toxicity, and good potentiation (4−4096-fold). The best adjuvant, **NAda**, showed as high as 4096-fold potentiation and rejuvenated the efficacy of different classes of antibiotics. Weak membrane perturbation was a combination of slight outer-membrane permeabilization and slight membrane depolarization and was also sufficient to inhibit the efflux machinery in bacteria. Compounds with acyclic aliphatic hydrophobic groups were moderately membrane-perturbing and toxic at potentiating concentrations. Strong, moderate, and weak membrane perturbation of compounds was also confirmed through the leakage of carboxyfluorescein from mammalian and bacterial mimics of liposomes. The cyclic hydrophobic analogues, **NAda** and **NDiphe**, led to no leakage of carboxyfluorescein from the liposomes, signifying their weak membrane-perturbing nature. Mitochondrial membrane depolarization at nontoxic concentrations of acyclic aliphatic analogues deemed them as misfits for the choice of antibiotic adjuvants. On the contrary, no significant mitochondrial membrane depolarization was observed for the cyclic hydrophobic analogues. The topmost critical pathogens including NDM-1-producing bacteria were found to be inactivated using combinations of various antibiotics with **NAda** and **NDiphe**. Multiple classes of antibiotics, which are usually rendered ineffective due to the permeability barrier or efflux pumps, like glycopeptides, tetracyclines, macrolides, rifamycins, fusidic acid, and chloramphenicol, were potentiated in the presence of the lead adjuvant.

In conclusion, we established, for the first time, that only weak but not strong membrane perturbation is ideal for designing a nontoxic and nonactive adjuvant for nonspecific potentiation of antibiotics. This is true as unnecessary extensive membrane perturbation and toxicity might result from higher-chain acyclic aliphatic analogues. These nontoxic small-molecular adjuvants and insights into their mechanism of action are an asset amidst the growing problem of AMR. This study will be helpful in aiding solutions to the problems in the clinical translation of membrane-targeting compounds, which are often toxic due to extensive membrane disruption. Moreover, these nontoxic adjuvants will be able to rejuvenate the efficacy of obsolete antibiotics, thus reinstating the potential of the existing antibiotic arsenal.

METHODS

Instrumentation and Materials. Reagent-grade solvents were used, which were distilled and dried before their use unless stated otherwise. All of the reagents were purchased from Sigma-Aldrich, Alfa−Aesar, S.D. Fine Chem. Limited, and Spectrochem. They were used without further purification. E. Merck TLC plates precoated with silica gel 60 F254 were used for thin-layer chromatography (TLC). UV light and iodine were used for visualization. For column chromatography, 60−120-mesh silica gel was used with varying ratios of chloroform and methanol solvent system as the eluent. A Bruker (AV-400) 400 MHz spectrometer was used for recording nuclear magnetic resonance spectra in deuterated solvents. 6538 UHD Accurate-Mass Q-TOF LC-MS instrument from Agilent Technologies was used for high-resolution mass spectrometry (HRMS). The Analytical HPLC Model 1260 Infinity II with VWD & Fraction Collector from Agilent Technologies was used for RP-HPLC. In the biological assays, the Tecan Infinite Pro series M200 Microplate Reader was used for measurement of optical density. Multidrug-resistant bacterial strains, namely, *A. baumannii* R674, *P. aeruginosa* R590, *Escherichia coli* R3336, and *K. pneumoniae* R3934, were obtained from NIMHANS, Bengaluru, India. Two strains among these, *E. coli* R3336 and *K. pneumoniae* R3934, were NDM-positive strains.

Synthesis. *Synthesis of N^1-Boc-N^3-(3-(Boc-amino)-propyl)propane-1,3-diamine (**1a**).* The compound was synthesized as previously reported.[18] Briefly, norspermidine (10 g, 1 equiv, 76.27 mmol) was dissolved in MeOH (50 mL) and the solution was kept at −80 °C. Boc anhydride (∼25 g, 1.5 equiv, 114.31 mmol) in MeOH (50 mL) was added to the reaction mixture dropwise. The reaction was allowed to happen for 1 h at −80 °C. After the reaction mixture reached RT, MeOH was removed and a pure compound was obtained through column chromatography on 60−120-mesh silica gel using methanol and chloroform (7:93) as the eluent. A colorless product, sticky in nature, with 50% yield was obtained. The detailed molecular characterization is provided in the Supporting Information.

*Procedure for Synthesizing **1b−1e**.*[18] About 1.2 equiv of saturated aliphatic acid (decanoic, dodecanoic) and carboxylic acids with aromatic radicals (naphthylacetic, diphenylpropanoic acid) were dissolved in 12 mL of DCM at 0 °C. Then, 3 equiv of diisopropylethyl amine (DIPEA) was put in the reaction mixture followed by 1.2 equiv of *N,N,N′,N′*-tetramethyl-*O*-(1*H*-benzotriazol-1-yl) uronium hexafluorophosphate (HBTU). dimethylformamide (DMF) (3 mL) was added to dissolve the HBTU in the reaction mixture. After 10 min, 1 equiv of **1a** in DCM (1 mL) was added dropwise to the reaction mixture. The reaction was allowed to happen for 24 h at RT. After evaporation of the solvent, the residue was diluted in ethyl acetate. Then, a workup was carried out at first with 1 N HCl multiple times, followed by a saturated sodium carbonate solution. The crude product was extracted in an ethyl acetate layer. The ethyl acetate layer was passed through anhydrous Na_2SO_4 to remove the water. Column chromatography was performed on 60−120-mesh silica gel using different ratios of methanol and chloroform as the eluent. **1b−1e** were obtained with 55−90% yield. The detailed characterization is provided in the Supporting Information.

*Synthesis of N-(Adamantan-2-yl)-2-bromoethanamide (**1f**).* About 500 mg of 2-adamantyl amine hydrochloride (1 equiv, 2.66 mmol) was dissolved in 12 mL of DCM (nondried), and 552 mg of K_2CO_3 (1.5 equiv, 3.99 mmol) dissolved in 10 mL of water was added to it at 5 °C. Bromoacetyl bromide (806.5 mg, 1.5 equiv, 3.99 mmol) was dissolved in 8 mL of DCM and slowly added to the reaction mixture using a dropper funnel. Until the addition of bromoacetyl bromide, the reaction was kept at 5 °C and then at room temperature for 12 h. After 12 h, the reaction was stopped, the DCM layer was collected and worked up with water 3 times, and finally evaporated to get the desired pure product with 85% yield. The characterization is provided in the Supporting Information.

*Synthesis of N-(Adamantan-2-yl)-2-[N′,N′-{bis-(3-boc-amino)propyl}amino] Ethanamide (**1g**).* N^1-Boc-N^3-(3-(Boc-amino)-propyl)propane-1,6-diamine, **1a** (300 mg, 1 equiv, 0.905 mmol), was dissolved in DMF. K_2CO_3 (187.6 mg, 1.5 equiv, 1.36 mmol) was added to the reaction mixture. Then, 246.33 mg of *N*-(adamantan-2-yl)-2-bromoethanamide, **1f** (1 equiv, 0.905 mmol), dissolved in DMF was added to the reaction mixture. The reaction was stirred at room temperature

https://doi.org/10.1021/acsinfecdis.2c00092
ACS Infect. Dis. 2022, 8, 1086−1097

for 24 h. The reaction mixture was then dissolved in ethyl acetate, and workup was performed with ice-cold water (3 times) to remove the DMF. The ethyl acetate layer was collected and passed through anhydrous Na_2SO_4, and the solvent was evaporated to get the pure product with 80% yield. The detailed characterization is provided in the Supporting Information.

Procedure for Synthesizing Final Compounds (NC10, NC12, NNaph, NDiphe, NAda).[18] At first, 1 equiv of **1b−1e** and **1g** was dissolved in DCM. Then, 4 equiv (excess amount) of trifluoroacetic acid (TFA) was added to the reaction mixture and allowed to stir at RT for 4 h. After that, the solvent and unused TFA were removed to get the pure product with a quantitative yield. The characterization details are given in the Supporting Information. The purity of all final compounds was >95%, determined using reverse phase-high performance liquid chromatography (RP-HPLC).

Biophysical and Biological Assays. *Investigation of Membrane-Perturbing Properties. Outer-Membrane Permeabilization Assay.*[19] Mid-log-phase bacterial cells (~10^8 CFU/mL) were grown. After washing the cells with 5 mM HEPES and 5 mM glucose, they were resuspended in a 1:1 solution of the same. To this suspension, *N*-phenylnaphthylamine dye was added to make a final concentration of 10 μM. Then, 180 μL of this dye-containing suspension was added to the wells of a 96-well plate (black wells, clear bottom) and stabilized for a few minutes. Then, 20 μL of the compounds and CTAB were added to the solution to maintain a final concentration of 100 μg/mL (50 and 25 μg/mL CTAB were also used given its high activity, but the results were similar). After addition, the fluorescence intensity ($\lambda_{excitation}$ = 350 nm; $\lambda_{emission}$ = 420 nm) was measured every 2 min for about 40 min. The fluorescence intensity at the end of 40 min was plotted for all compounds in Figure 1A.

Cytoplasmic Membrane Depolarization Assay.[19] Mid-log-phase bacterial cells (~10^8 CFU/mL) were grown and washed with 5 mM HEPES and 5 mM glucose. Bacterial cells were reconstituted in a 1:1:1 solution of 5 mM glucose, 5 mM HEPES, and 100 mM KCl solution. $DisC_3(5)$ was added to this suspension to make a final concentration of 2 μM. After preincubation for 40 min in the wells of a black 96-black-well plate, the fluorescence of the bacterial suspension was measured ($\lambda_{excitation}$ = 622 nm; $\lambda_{emission}$ = 670 nm) and allowed to stabilize for a few minutes at RT. Then, 20 μL of compounds and CTAB was added to the wells to maintain a final concentration of 100 μg/mL (50 and 25 μg/mL CTAB was also used given its high activity, but the results were similar). Fluorescence intensity was measured every 2 min for about 40 more minutes. The fluorescence intensity at the end of 40 min was plotted for all compounds in Figure 1A.

In Vitro Antibacterial Assays. Antibacterial Activity in Broth Culture Media.[33] Antibacterial activity was determined by slightly modifying the standardized protocols.[32] The detailed protocol is given in the Supporting Information.

Potentiation Efficacy of Adjuvants-Chequerboard Assays.[19] The potentiation efficacy of adjuvants with antibiotics was measured in Mueller Hinton broth media using the well-known chequerboard assays. A solution of 25 μL each of antibiotic and adjuvants of concentrations varying 2-fold, starting with 64−128 μg/mL for antibiotic and 128 μg/mL for adjuvant, was added into each well of a 96-well plate followed by 150 μL of a bacterial suspension (~10^5 CFU/mL) and incubated at 37 °C for 18−24 h. Bacterial suspension alone and Mueller Hinton broth alone served as positive and negative growth controls, respectively. The assays were performed twice.

Assay for In Vitro Mammalian Cell Toxicity. Hemolytic Assay.[18] A previously reported protocol was followed. The detailed protocol is provided in the Supporting Information.

Lactic Acid Dehydrogenase (LDH) Assay.[18] A previously reported protocol was followed. The detailed protocol is provided in the Supporting Information.

MTT Assay. A similar protocol was followed as in the LDH assay except for the fact that the MTT reagent {3-(4,5-dimethylthiazol-2-yl)-2,5-diphenyl tetrazolium bromide} was added to the wells after 24 h of treatment with compound solutions (starting from the concentration of 512 μg/mL). The detailed protocol is given in the Supporting Information.

Carboxyfluorescein Assay.[34] To investigate dye leakage by compounds using fluorescence spectroscopy, vesicles entrapped with 30 mM 5(6)-carboxyfluorescein dye were prepared in 1× phosphate-buffered saline (PBS) buffer.[34] 5(6)-Carboxyfluorescein has an excitation maximum at 492 nm and an emission maximum at 517 nm. For the dye leakage studies, the change in concentration of the dye was monitored by measuring the fluorescence intensity keeping the excitation at 492 nm and emission at 517 nm. The 5(6)-carboxyfluorescein dye-entrapped bacterial mimic vesicles were prepared from DPPG lipid and DPPE lipid (88:12)[35] in a 5(6)-carboxyfluorescein solution (30 mM) in 1× PBS buffer. The same vesicles for mammalian mimic were prepared from the DPPC lipid in a 5(6)-carboxyfluorescein solution (30 mM) in 1× PBS buffer. 5(6)-Carboxyfluorescein dye was removed from the extravesicular solution using size exclusion chromatography. Sephadex G-50 was used as the stationary phase, and 1× PBS buffer was used as the eluent. For the fluorescence experiment, the vesicles were equilibrated with 1× PBS buffer, following which compound solutions in water were added to make the final concentration 320 μg/mL. The control experiment was done upon addition of water instead of the compound solution. Dye leakage was gauged by monitoring the fluorescence intensity due to 5(6)-carboxyfluorescein dye leakage, which decreases the concentration of the dye. To cleave the vesicle, 1% Triton-X was used to give a 3 mM dye concentration, which leads to the final fluorescence value. The fluorescence intensity was normalized based on the final values. The curves were fitted using OriginPro 8.5 software.

Flow Cytometry.[36] The assay was performed using a modified protocol.[36] In brief, HEK 293 cells were seeded in 12-well plates at a concentration of 5 × 10^5 cells/well. After 24 h of cell attachment, compound solutions were added at nontoxic concentrations (1−100 μg/mL). Two wells were left untreated for the CCCP treatment (final concentration = 50 μM or 10 μg/mL), which was given just 5 min before JC-1 dye addition. For the rest of the wells, the media was removed after 24 h, washed twice with 1× PBS, and JC-1 dye was added to a final concentration of 2 μM in 1× PBS. The cells were incubated with the dye for 30 min at 37 °C at 5% CO_2. The extra dye was removed after centrifuging the cells at 300 rpm, and fresh 1× PBS was added. The solutions were taken for analysis in a flow cytometer (BD Biosciences) using an excitation wavelength of 488 nm and appropriate emission filters for R-phycoerythrin and fluorescein isothiocyanate (FITC). Gating and analysis were done using FCS Express 6 software.

https://doi.org/10.1021/acsinfecdis.2c00092
ACS Infect. Dis. 2022, 8, 1086−1097

Confocal Laser Scanning Microscopy (CLSM). HEK 293 cells were seeded at a density of 5 $\times 10^5$ cells in customized Petri dishes with an 18 mm glass bottom. After 24 h of cell attachment, compound solutions were added at various nontoxic concentrations (1−100 μg/mL). A similar protocol was followed as in the case of flow cytometry. After incubating with JC-1 dye (2 μM) for 30 min, the 1× PBS solution was changed and the cells were imaged using a Zeiss 510 Meta confocal laser scanning microscope by exciting at 488 nm and checking the emission at 530 nm (monomer) and 590 nm (*J*-aggregates). The images were processed using an LSM 5 Image examiner.

Antibiotic Accumulation Assay.[19] A mid-log-phase culture of *E. coli* R3336 and *K. pneumoniae* R3934 was centrifuged (at 9000 rpm for 5 min) and washed in 10 mM HEPES buffer. The bacterial cells were resuspended to ∼10^8 CFU/mL in 10 mM HEPES buffer with 128 μg/mL minocycline. After this, 190 μL of this minocycline-containing bacterial suspension was added into the wells of a black 96-well plate with a clear bottom. The fluorescence was recorded for a few minutes ($\lambda_{excitation}$ = 405 nm; $\lambda_{emission}$ = 535 nm). After that, 10 μL of **NAda** or **NDiphe** was added to the wells to make a final concentration of 100 μg/mL. Fluorescence was monitored for about 30−40 min. A total of 10 μL of Millipore water added to the minocycline-containing suspension was used as the negative control. The experiment was performed in triplicate, and the average data was plotted. The increased accumulation of minocycline in the bacterial cells was indicated by an augmentation in the minocycline fluorescence intensity.

EtBr Efflux Assay.[37] A freshly grown mid-log-phase culture of bacterial cells was centrifuged (9000 rpm for 5 min) and resuspended in MHB. Bacterial cells (∼10^8 CFU/mL) were coincubated with 5 μM EtBr for 1 h at 37 °C and 150 rpm. The cells were centrifuged (9000 rpm for 5 min), washed to remove excess EtBr, and resuspended in fresh MHB. The inoculum was adjusted to OD_{600} of 0.4. Then, 180 μL of the bacterial inoculum was added into 96-well, black-well, clear-bottom plates and 20 μL of CCCP or **NAda**/**NDiphe** was added to final concentrations of 20 and 100 μg/mL. Then, 20 μL of Millipore water was added to the untreated controls, and wells with bacteria without EtBr were taken as the negative control. EtBr efflux from the cells was monitored with the excitation wavelength at 530 nm and emission wavelength at 600 nm for 40 min. EtBr fluorescence was used to determine the activity of efflux pumps like AcrAB-TolC in bacteria. The experiment was independently performed twice with three technical replicates each time. The average data was plotted.

■ ASSOCIATED CONTENT

Supporting Information

The Supporting Information is available free of charge at https://pubs.acs.org/doi/10.1021/acsinfecdis.2c00092.

Characterization details, characterization spectra, experimental protocols, tables about activity and potentiation of antibiotics by adjuvants, chequerboards of combinations, microscopy images of mitochondrial membrane depolarization, temporal uptake of antibiotic in the presence of adjuvants, trends of potentiation factors, and membrane perturbation graphs and chequerboards showing ubiquitous potentiation of antibiotics (PDF)

■ AUTHOR INFORMATION

Corresponding Author

Jayanta Haldar − *Antimicrobial Research Laboratory, New Chemistry Unit and School of Advanced Materials, Jawaharlal Nehru Centre for Advanced Scientific Research (JNCASR), Bengaluru 560064 Karnataka, India;* orcid.org/0000-0002-8068-1015; Phone: (+91) 80-2208-2565; Email: jayanta@jncasr.ac.in; Fax: (+91) 80-2208-2627

Authors

Geetika Dhanda − *Antimicrobial Research Laboratory, New Chemistry Unit, Jawaharlal Nehru Centre for Advanced Scientific Research (JNCASR), Bengaluru 560064 Karnataka, India*

Riya Mukherjee − *Antimicrobial Research Laboratory, New Chemistry Unit, Jawaharlal Nehru Centre for Advanced Scientific Research (JNCASR), Bengaluru 560064 Karnataka, India*

Debajyoti Basak − *Antimicrobial Research Laboratory, New Chemistry Unit, Jawaharlal Nehru Centre for Advanced Scientific Research (JNCASR), Bengaluru 560064 Karnataka, India*

Complete contact information is available at: https://pubs.acs.org/10.1021/acsinfecdis.2c00092

Author Contributions

G.D. conceived the project, designed all of the experiments, performed synthesis, characterization, and *in vitro* assays, collected data, analyzed the results, and wrote the manuscript. R.M. and G.D. performed mitochondrial membrane depolarization studies through flow cytometry and confocal microscopy. R.M. performed cell culture experiments. D.B. and G.D. performed liposome dye leakage experiments. J.H. designed the project, supervised the research, and wrote the manuscript.

Notes

The authors declare no competing financial interest.

■ ACKNOWLEDGMENTS

J.H. acknowledges SERB (CRG/2020/003118), Govt. of India, and DBT (BT/PR31801/MED/29/1394/2019) for financial support.

■ REFERENCES

(1) O'Neill, J. *Tackling Drug-Resistant Infections Globally: Final Report and Recommendations*; 2016; pp 1−84.

(2) WHO. Global Priority List of Antibiotic-Resistant Bacteria to guide Research, Discovery, and Development of New Antibiotics, 2017. https://www.who.int/news/item/27-02-2017-who-publishes-list-of-bacteria-for-which-new-antibiotics-are-urgently-needed (accessed January 28, 2022).

(3) Westblade, L. F.; Simon, M. S.; Satlin, M. J. Bacterial Coinfections in Coronavirus Disease 2019. *Trends Microbiol.* **2021**, *29*, 930−941.

(4) Breijyeh, Z.; Jubeh, B.; Karaman, R. Resistance of Gram-Negative Bacteria to Current Antibacterial Agents and Approaches to Resolve It. *Molecules* **2020**, *25*, No. 1340.

(5) Du, D.; Wang-Kan, X.; Neuberger, A.; van Veen, H. W.; Pos, K. M.; Piddock, L. J. V.; Luisi, B. F. Multidrug efflux pumps: structure, function and regulation. *Nat. Rev. Microbiol.* **2018**, *16*, 523−539.

(6) Paulsen, I. T.; Brown, M. H.; Skurray, R. A. Proton-dependent multidrug efflux systems. *Microbiol. Rev.* **1996**, *60*, 575−608.

(7) Tyers, M.; Wright, G. D. Drug combinations: a strategy to extend the life of antibiotics in the 21st century. *Nat. Rev. Microbiol.* **2019**, *17*, 141−155.
(8) Wright, G. D. Antibiotic Adjuvants: Rescuing Antibiotics from Resistance. *Trends Microbiol.* **2016**, *24*, 862−871.
(9) Song, M.; Liu, Y.; Huang, X.; Ding, S.; Wang, Y.; Shen, J.; Zhu, K. A broad-spectrum antibiotic adjuvant reverses multidrug-resistant Gram-negative pathogens. *Nat. Microbiol.* **2020**, *5*, 1040−1050.
(10) Hurdle, J. G.; O'Neill, A. J.; Chopra, I.; Lee, R. E. Targeting bacterial membrane function: an underexploited mechanism for treating persistent infections. *Nat. Rev. Microbiol.* **2011**, *9*, 62−75.
(11) Cai, J.; Wei, L. Editorial of Special Column "Novel Peptides and Peptidomimetics in Drug Discovery". *Acta Pharm. Sin. B* **2021**, *11*, 2606−2608.
(12) Douafer, H.; Andrieu, V.; Phanstiel, O.; Brunel, J. M. Antibiotic Adjuvants: Make Antibiotics Great Again! *J. Med. Chem.* **2019**, *62*, 8665−8681.
(13) French, S.; Farha, M.; Ellis, M. J.; Sameer, Z.; Cote, J. P.; Cotroneo, N.; Lister, T.; Rubio, A.; Brown, E. D. Potentiation of Antibiotics against Gram-Negative Bacteria by Polymyxin B Analogue SPR741 from Unique Perturbation of the Outer Membrane. *ACS Infect. Dis.* **2020**, *6*, 1405−1412.
(14) Konai, M. M.; Haldar, J. Lysine-Based Small Molecule Sensitizes Rifampicin and Tetracycline against Multidrug-Resistant *Acinetobacter baumannii* and *Pseudomonas aeruginosa*. *ACS Infect. Dis.* **2020**, *6*, 91−99.
(15) Stokes, J. M.; MacNair, C. R.; Ilyas, B.; French, S.; Cote, J. P.; Bouwman, C.; Farha, M. A.; Sieron, A. O.; Whitfield, C.; Coombes, B. K.; Brown, E. D. Pentamidine sensitizes Gram-negative pathogens to antibiotics and overcomes acquired colistin resistance. *Nat. Microbiol.* **2017**, *2*, No. 17028.
(16) MacNair, C. R.; Stokes, J. M.; Carfrae, L. A.; Fiebig-Comyn, A. A.; Coombes, B. K.; Mulvey, M. R.; Brown, E. D. Overcoming mcr-1 mediated colistin resistance with colistin in combination with other antibiotics. *Nat. Commun.* **2018**, *9*, No. 458.
(17) Farha, M. A.; French, S.; Stokes, J. M.; Brown, E. D. Bicarbonate Alters Bacterial Susceptibility to Antibiotics by Targeting the Proton Motive Force. *ACS Infect. Dis.* **2018**, *4*, 382−390.
(18) Konai, M. M.; Ghosh, C.; Yarlagadda, V.; Samaddar, S.; Haldar, J. Membrane active phenylalanine conjugated lipophilic norspermidine derivatives with selective antibacterial activity. *J. Med. Chem.* **2014**, *57*, 9409−9423.
(19) Uppu, D. S. S. M.; Manjunath, G. B.; Yarlagadda, V.; Kaviyil, J. E.; Ravikumar, R.; Paramanandham, K.; Shome, B. R.; Haldar, J. Membrane-active macromolecules resensitize NDM-1 gram-negative clinical isolates to tetracycline antibiotics. *PLoS One* **2015**, *10*, No. e0119422.
(20) Kashket, E. R. The proton motive force in bacteria: a critical assessment of methods. *Annu. Rev. Microbiol.* **1985**, *39*, 219−242.
(21) Helander, I. M.; Mattila-Sandholm, T. Fluorometric assessment of gram-negative bacterial permeabilization. *J. Appl. Microbiol.* **2000**, *88*, 213−219.
(22) Laws, M.; Shaaban, A.; Rahman, K. M. Antibiotic resistance breakers: current approaches and future directions. *FEMS Microbiol. Rev.* **2019**, *43*, 490−516.
(23) Nolivos, S.; Cayron, J.; Dedieu, A.; Page, A.; Delolme, F.; Lesterlin, C. Role of AcrAB-TolC multidrug efflux pump in drug-resistance acquisition by plasmid transfer. *Science* **2019**, *364*, 778−782.
(24) de Cristóbal, R. E.; Vincent, P. A.; Salomón, R. A. Multidrug resistance pump AcrAB-TolC is required for high-level, Tet(A)-mediated tetracycline resistance in *Escherichia coli*. *J. Antimicrob. Chemother.* **2006**, *58*, 31−36.
(25) Zorova, L. D.; Popkov, V. A.; Plotnikov, E. Y.; Silachev, D. N.; Pevzner, I. B.; Jankauskas, S. S.; Babenko, V. A.; Zorov, S. D.; Balakireva, A. V.; Juhaszova, M.; Sollott, S. J.; Zorov, D. B. Mitochondrial membrane potential. *Anal. Biochem.* **2018**, *552*, 50−59.
(26) Horvath, S. E.; Daum, G. Lipids of mitochondria. *Prog. Lipid Res.* **2013**, *52*, 590−614.
(27) Yamaguchi, A.; Ohmori, H.; Kaneko-Ohdera, M.; Nomura, T.; Sawai, T. Delta pH-dependent accumulation of tetracycline in *Escherichia coli*. *Antimicrob. Agents Chemother.* **1991**, *35*, 53−56.
(28) Du, D.; Wang-Kan, X.; Neuberger, A.; van Veen, H. W.; Pos, K. M.; Piddock, L.J.V.; Luisi, B. F. Multidrug efflux pumps: structure, function and regulation. *Nat. Rev. Microbiol.* **2018**, *16*, 523−539.
(29) Martins, M.; McCusker, M. P.; Viveiros, M.; Couto, I.; Fanning, S.; Pages, J. M.; Amaral, L. A Simple Method for Assessment of MDR Bacteria for Over-Expressed Efflux Pumps. *Open Microbiol. J.* **2013**, *7*, 72−82.
(30) Sanchez-Carbonel, A.; Mondragón, B.; López-Chegne, N.; Peña-Tuesta, I.; Huayan-Dávila, G.; Blitchtein, D.; Carrillo-Ng, H.; Silva-Caso, W.; Aguilar-Luis, M. A.; Valle-Mendoza, J. D. The effect of the efflux pump inhibitor Carbonyl Cyanide m-Chlorophenylhydrazone (CCCP) on the susceptibility to imipenem and cefepime in clinical strains of *Acinetobacter baumannii*. *PLoS One* **2021**, *16*, No. e0259915.
(31) Linciano, P.; Cendron, L.; Gianquinto, E.; Spyrakis, F.; Tondi, D. Ten Years with New Delhi Metallo-β-lactamase-1 (NDM-1): From Structural Insights to Inhibitor Design. *ACS Infect. Dis.* **2019**, *5*, 9−34.
(32) Nakajima, Y. Mechanisms of bacterial resistance to macrolide antibiotics. *J. Infect. Chemother.* **1999**, *5*, 61−74.
(33) Wiegand, I.; Hilpert, K.; Hancock, R. E. Agar and broth dilution methods to determine the minimal inhibitory concentration (MIC) of antimicrobial substances. *Nat. Protoc.* **2008**, *3*, 163−175.
(34) He, R.; Bonaventura, I. D.; Visini, R.; Gan, B.-H.; Fu, Y.; Probst, D.; Lüscher, A.; Köhler, T.; van Delden, C.; Stocker, A.; Hong, W.; Darbre, T.; Reymond, J.-L. Design, crystal structure and atomic force microscopy study of thioether ligated d,l-cyclic antimicrobial peptides against multidrug resistant *Pseudomonas aeruginosa*. *Chem. Sci.* **2017**, *8*, 7464−7475.
(35) Konai, M. M.; Samaddar, S.; Bocchinfuso, G.; Santucci, V.; Stella, L.; Haldar, J. Selectively targeting bacteria by tuning the molecular design of membrane-active peptidomimetic amphiphiles. *Chem. Commun.* **2018**, *54*, 4943−4946.
(36) Sivandzade, F.; Bhalerao, A.; Cucullo, L. Analysis of the Mitochondrial Membrane Potential Using the Cationic JC-1 Dye as a Sensitive Fluorescent Probe. *Bio-Protoc.* **2019**, *9*, No. e3128.
(37) Kaatz, G. W.; Seo, S. M.; O'Brien, L.; Wahiduzzaman, M.; Foster, T. J. Evidence for the existence of a multidrug efflux transporter distinct from NorA in Staphylococcus aureus. *Antimicrob. Agents Chemother.* **2000**, *44*, 1404−1406.

https://doi.org/10.1021/acsinfecdis.2c00092
ACS Infect. Dis. 2022, 8, 1086−1097

VIP Antibiotics Very Important Paper

International Edition: DOI: 10.1002/anie.201601621
German Edition: DOI: 10.1002/ange.201601621

A Vancomycin Derivative with a Pyrophosphate-Binding Group: A Strategy to Combat Vancomycin-Resistant Bacteria

*Venkateswarlu Yarlagadda, Paramita Sarkar, Sandip Samaddar, and Jayanta Haldar**

Abstract: *Vancomycin, the drug of last resort for Gram-positive bacterial infections, has also been rendered ineffective by the emergence of resistance in such bacteria. To combat the threat of vancomycin-resistant bacteria (VRB), we report the development of a dipicolyl–vancomycin conjugate (Dipi-van), which leads to enhanced inhibition of cell-wall biosynthesis in VRB and displays in vitro activity that is more than two orders of magnitude higher than that of vancomycin. Conjugation of the dipicolyl moiety, which is a zinc-binding ligand, endowed the parent drug with the ability to bind to pyrophosphate groups of cell-wall lipids while maintaining the inherent binding affinity for pentapeptide termini of cell-wall precursors. Furthermore, no detectable resistance was observed after several serial passages, and the compound reduced the bacterial burden by a factor of 5 logs at 12 mg kg^{-1} in a murine model of VRB kidney infection. The findings presented in this report stress the potential of our strategy to combat VRB infections.*

Vancomycin, a clinically important glycopeptide antibiotic, has been the antibiotic of last resort for the treatment of drug-resistant Gram-positive bacterial infections, particularly of those resistant to β-lactam antibiotics, such as methicillin-resistant *Staphylococcus aureus* (MRSA).[1] The increased use of vancomycin against prevailing MRSA strains has led to the emergence of vancomycin-intermediate-resistant *S. aureus* (VISA) and vancomycin-resistant *S. aureus* (VRSA).[2] Furthermore, vancomycin-resistant *Enterococci* (VRE) have become one of the most common hospital-acquired pathogens, and constitute a global health concern.[3] At present, the treatment options for these drug-resistant infections are severely limited, and only a few drugs, such as daptomycin, quinupristin/dalfopristin, and linezolid, are available.[4,5] Bacteria have already started acquiring resistance even to these last-line antibiotics in clinical settings.[4,5] This poses a major health problem and has stimulated efforts to develop various strategies to combat drug-resistant pathogens.[6–12]

Vancomycin inhibits the cell-wall biosynthesis of Gram-positive bacteria by specifically binding to the D-Ala-D-Ala terminal of the cell-wall precursor pentapeptide, thus inhibiting transpeptidase-catalyzed cross-linking and maturation of the bacterial cell wall.[1] Bacteria acquired resistance to vancomycin by remodeling their cell-wall precursors that terminate in the D-Ala-D-Lac (lactate) depsipeptide, which reduces the vancomycin binding affinity by a factor of about 1000 and allows for unimpeded peptide-chain cross-linking (VanA and VanB phenotypes of vancomycin-resistant bacteria (VRB)).[13] Several strategies have been developed to combat bacterial resistance towards vancomycin. These involve either enhancing the binding affinity of the drug for bacterial ligands or installing membrane disruption properties, an additional mechanism of action, to vancomycin.[14,15]

The bacterial cell wall (peptidoglycan) is a three-dimensional network of long aminosugar strands (*N*-acetylmuramic acid, NAM; *N*-acetylglucosamine, NAG) cross-linked by a pentapeptide that is located on the exterior of the cytoplasmic membrane. Peptidoglycan subunits are assembled at the extracellular surface on a membrane-embedded polyisoprenoid anchor, such as bactoprenol pyrophosphate and lipid II (undecaprenyl-pyrophosphoryl-NAM-NAG-pentapeptide).[1] As these cell-wall lipids are essential for cell-wall biosynthesis, they represent attractive targets for antibacterial compounds, such as bacitracin, glycopeptides, mannopeptimycins, and several lantibiotics.[16] It has been shown that dipicolyl–Zn^{2+} complexes have a high affinity to complexation with pyrophosphates.[17] Generally, the concentration of divalent zinc ions (Zn^{2+}) in bacteria is about 100 μM, and their concentration is expected to increase in response to inflammation at the bacterial infection site as a consequence of Zn^{2+} release from damaged or apoptotic cells (ca. 100 μM).[18] As cell-wall lipids are present in the periplasmic space, we hypothesized that a dipicolyl derivative of vancomycin, Dipi-van, which can chelate Zn^{2+} (for example, from bacterial sources), can result in the formation of Dipi-van–Zn^{2+} complexes with the pyrophosphates of cell-wall lipids. Furthermore, we anticipated that this complex will not only maintain its inherent binding affinity towards pentapeptide termini but also have the ability to bind to the pyrophosphate groups of cell-wall lipids, which may result in enhanced inhibition of cell-wall biosynthesis. Herein, dipicolyl-1,6-hexadiamine (Dipi) was conjugated to vancomycin to yield a dipicolyl–vancomycin conjugate (Dipi-van). Dipi-van was found to be 375-fold more effective than vancomycin against VRE (VanA phenotype). Unlike vancomycin, Dipi-van did not induce the development of bacterial resistance. Compared to vancomycin, Dipi-van showed a higher in vivo antibacterial activity against VRE in a murine kidney infection model with no toxicity observed under the conditions used.

Dipi-van (**4**) was prepared in 77% yield by coupling the carboxylic group of vancomycin to dipicolyl-substituted 1,6-

[*] Dr. V. Yarlagadda, P. Sarkar, Dr. S. Samaddar, Dr. J. Haldar
Chemical Biology and Medicinal Chemistry Laboratory
New Chemistry Unit
Jawaharlal Nehru Centre for Advanced Scientific Research (JNCASR)
Jakkur, Bengaluru 560064, Karnataka (India)
E-mail: jayanta@jncasr.ac.in

Supporting information for this article can be found under: http://dx.doi.org/10.1002/anie.201601621.

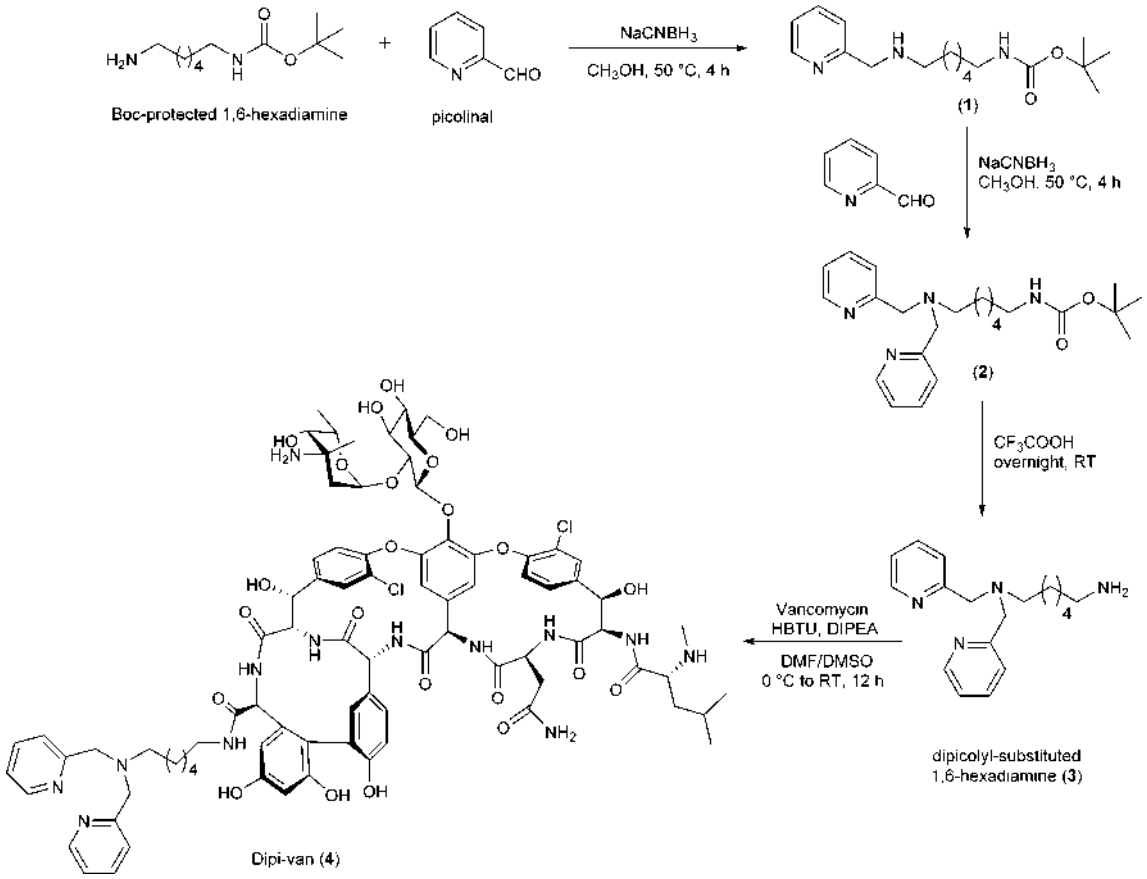

Scheme 1. Synthesis of Dipi-van (**4**). DIPEA = *N*,*N*-diisopropylethylamine, HBTU = *O*-(benzotriazol-l-yl)-*N*,*N*,*N*′,*N*′-tetramethyluronium hexafluorophosphate.

hexadiamine (Dipi, **3**) through an amide coupling with HBTU (Scheme 1). To synthesize **3**, mono-Boc-protected 1,6-hexadiamine was reacted twice with 2-picolinal (pyridine-2-aldehyde) to form the corresponding Schiff bases followed by reduction with sodium cyanoborohydride (compounds **1** and **2**). Then, the Boc group was removed under acidic conditions (Scheme 1) to yield dipicolyl-1,6-hexadiamine (**3**), which was directly used in the coupling with vancomycin. To prepare Dipi-van, vancomycin was dissolved in dry DMF/DMSO (1:1), and a solution of HBTU in DMF was added dropwise at 0 °C. Subsequently, **3** was added to the vancomycin solution, and the reaction mixture was stirred at room temperature for 12 h. It was then purified by reverse-phase HPLC to more than 95 % purity and characterized by ^{1}H and ^{13}C NMR spectroscopy and high-resolution mass spectrometry.

The antibacterial activities of vancomycin and Dipi-van were evaluated by determining the minimum inhibitory concentrations (MICs) against vancomycin-resistant strains of *Staphylococci* (VISA) and *Enterococci* (VRE; VanA and VanB phenotypes). The results are summarized in Figure 1 A. Dipi-van exhibited improved antibacterial activity towards VISA (MIC ≈ 1 μM) compared to vancomycin (MIC of 13 μM). The activity of Dipi-van was found to be approximately 375-fold and 160-fold higher than that of vancomycin against VREm (VanA phenotype, *E. faecium*) and VREs (VanB phenotype, *E. faecalis*), respectively (Figure 1 A). The antibacterial activity of the dipicolyl moiety alone (without vancomycin, compound **3**) was evaluated against VREm (VanA phenotype), and the compound was found to be inactive even at 100 μM. Furthermore, the activity of a physical mixture of vancomycin and compound **3** was determined, and it was found to be inactive against VREm even up to individual concentrations of 50 μM (Dipi-van: MIC = 2 μM).

Next, the activity of Dipi-van against VREm was evaluated in the presence of external divalent zinc ions (added as zinc sulfate, $ZnSO_4$). Under these conditions, the activity of Dipi-van was higher by a factor of two to three than in the absence of external Zn^{2+}. This enhanced activity was attributed to the formation of Dipi-van–Zn^{2+} complexes, which presumably bind to the pyrophosphates of cell-wall lipids that are accessible at the extracellular surface, and thereby interfere with their action in the continuous cyclic process of the formation of peptidoglycan layers. The formation of Dipi-van–Zn^{2+} complexes was confirmed by mass spectrometry (see the Supporting Information, Figure S1).

To validate our hypothesis, we evaluated the ability of Dipi-van–Zn^{2+} to complex with geranyl pyrophosphate (GPP, as a model compound for the cell-wall lipids). Dipi-van–Zn^{2+} and GPP were mixed in a molar ratio of 1:1, and the resulting mixture was allowed to stand for two hours at room temperature. Then the solution was analyzed by mass spectrometry, and a peak corresponding to the Dipi-van–Zn–GPP complex

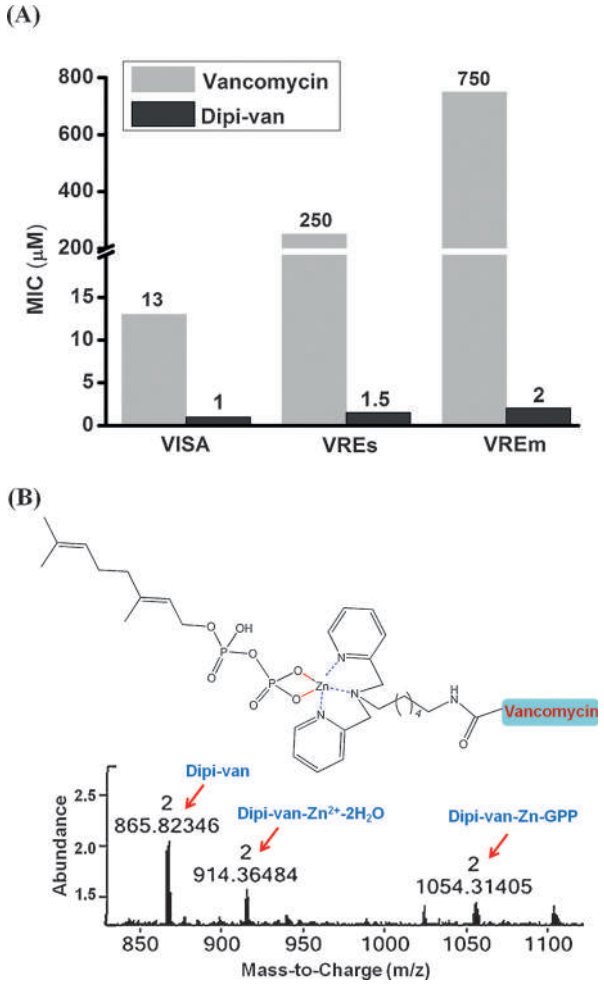

Figure 1. A) Antibacterial activity of Dipi-van and vancomycin against vancomycin-intermediate-resistant *S. aureus* (VISA), vancomycin-resistant *E. faecalis* (VREs, VanB phenotype), and vancomycin-resistant *E. faecium* (VREm, VanA phenotype). B) The complex of Dipi-van–Zn^{2+} with geranyl pyrophosphate (Dipi-van–Zn–GPP) was identified by mass spectrometry as indicated by the peak at *m/z* 1054.31. Dipi-van–Zn^{2+} can also coordinate two water molecules (*m/z* 914.36). In the presence of GPP, these water molecules are replaced by the pyrophosphate of GPP.

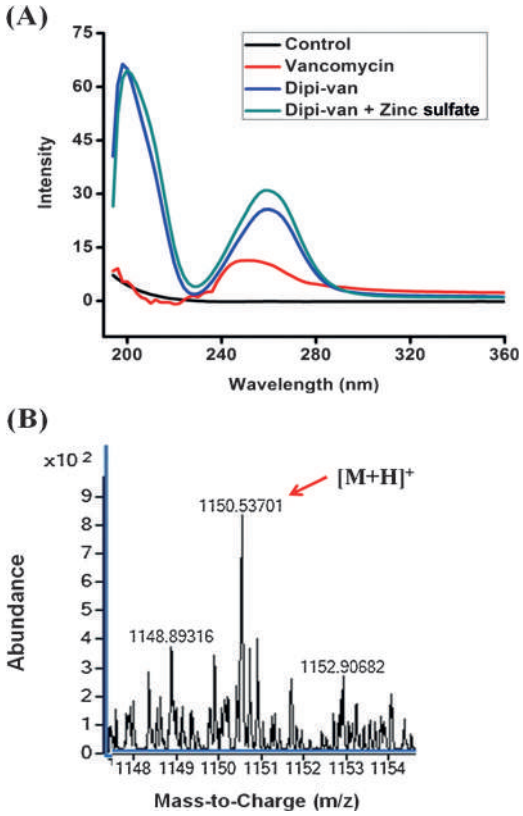

Figure 2. Inhibition of cell-wall biosynthesis: Intracellular accumulation of the cell wall precursor UDPMurNAc-pp after treatment of VREm (VanA phenotype) with vancomycin, Dipi-van, and Dipi-van in the presence of zinc sulfate at 5 μM. Untreated cells were used as the control. A) Identification of intracellular UDPMurNAc-pp by monitoring the absorbance at $\lambda = 260$ nm. B) UDPMurNAc-pp was identified by mass spectrometry (*m/z* 1150.53).

was observed, indicating the ability of the new glycopeptide to bind to pyrophosphate groups in cell-wall lipids (Figure 1 B). We evaluated the MIC of Dipi-van in the presence of molar equivalents of Zn^{2+} and GPP (as an antagonist) against VREm. In the presence of GPP, Dipi-van completely lost its activity owing to the formation of Dipi-van–Zn–GPP complexes. This finding further implies that Dipi-van can bind to the pyrophosphate groups of cell-wall lipids.

To investigate whether the new vancomycin derivative indeed has an inhibitory effect on cell-wall (peptidoglycan) biosynthesis, the accumulation of a UDP-linked peptidoglycan precursor,[19] UDP-*N*-acetylmuramyl-pentadepsipeptide (UDPMurNAc-pp), caused by treating VRE with 5 μM Dipi-van and vancomycin was compared through spectrophotometry (Figure 2 A and B). We also investigated the ability of Dipi-van to inhibit the cell-wall biosynthesis in the presence of external Zn^{2+}. Upon treatment with Dipi-van, a more intense peak was observed at 260 nm than for vancomycin treatment, which corresponds to the accumulation of UDP-MurNAc-pp and was confirmed by high-resolution mass spectrometry (*m/z* calcd for UDPMurNAc-pp ($C_{40}H_{64}N_8O_{27}P_2$): 1150.94 $[M+H]^+$; found: 1150.53). This result suggests that Dipi-van is a better inhibitor of cell-wall biosynthesis than vancomycin. Cell-wall biosynthesis was even more strongly inhibited by Dipi-van in the presence of Zn^{2+}. This result can be attributed to the ability of Dipi-van to bind to the pyrophosphates of cell-wall lipids, which is not possible with vancomycin. The cell-wall lipids are crucial for the formation of peptidoglycans as they translocate cell-wall intermediates (UDPMurNAc-pp) from intracellular to extracellular surfaces. Dipi-van presumably blocks the translocation and enhances the accumulation of UDPMurNAc-pp, which enhances the inhibition of cell-wall biosynthesis.

In the light of the alarming increase in drug resistance in bacteria, the potential emergence of bacterial resistance to this new compound was evaluated. The propensity of bacteria to generate resistance can be evaluated through serial exposure of the organisms to the antimicrobial agents. MRSA was thus exposed to vancomycin and Dipi-van for serial passages, and the changes in MIC values were monitored over a period of 25 days. Even after 25 serial

passages, the MIC of Dipi-van had remained the same (MIC ≈0.5 μM). However, in the case of vancomycin, the MIC value started to increase after seven passages, and the value had increased by a factor of 16 after 25 passages (Figure 3A). Thus bacteria have less propensity to develop resistance against this compound, which emphasizes the suitability of such compounds for clinical applications.

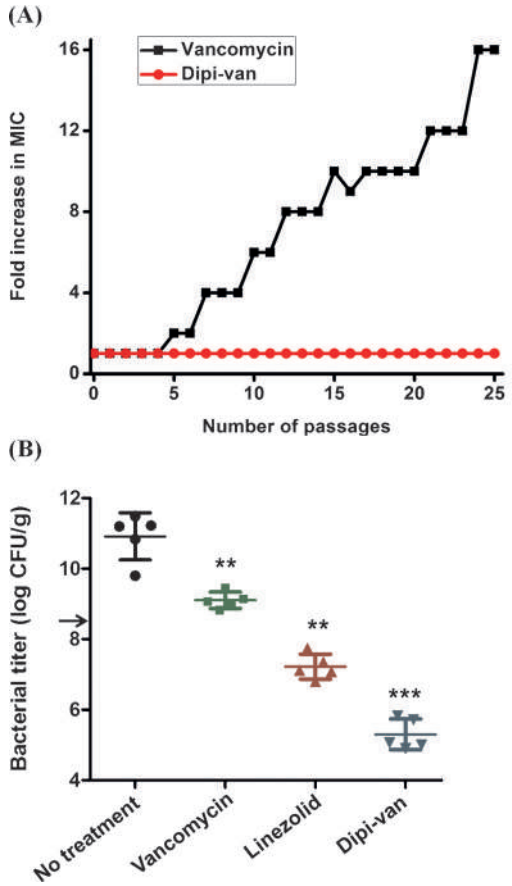

Figure 3. A) Development of bacterial resistance in MRSA towards vancomycin and Dipi-van. B) In vivo antibacterial activity of vancomycin, linezolid, and Dipi-van in a murine renal infection model against VRE at 12 mg kg^{-1}. The black arrow indicates the bacterial pre-treatment titer (ca. 8.0 $\log_{10}$ CFU g^{-1}). Five mice were used in each group. Statistical analysis was performed using Student's *t*-test. Differences are considered statistically significant from the untreated group with a value of $P<0.05$ with 95% confidence intervals (***$P<0.001$; **$P<0.01$).

The toxicity of Dipi-van was studied by measuring its hemolytic activity (HC_{50}; 50% hemolytic concentration) against human red blood cells (RBCs). Dipi-van did not show any significant toxicity towards the RBCs even at a concentration of 1000 μM, which indicates the selective toxicity of Dipi-van towards bacterial cells over mammalian cells. Next, the in vivo systemic toxicity of Dipi-van was assessed after single-dose intravenous (i.v.) administration to mice ($n=5$) at doses of 100 mg kg^{-1}. All of the mice were still alive after 14 days, indicating the high tolerability of Dipi-van in animals with $LD_{50}>100$ mg kg^{-1}.

Infections caused by VRE have been increasing, representing an emerging threat to public health.[3] The in vivo activity of Dipi-van was evaluated in a renal infection model against VRE. Initially, mice were injected intravenously with 0.2 mL of 0.2% λ-carrageenan to increase their susceptibility to bacterial renal infection. After seven days, the mice were infected with VRE (VanB phenotype, ca. 10^8 CFU/mouse; CFU = colony forming unit). After four hours, the mice were treated with three doses (at 24 h intervals) of vancomycin (12 mg kg^{-1}), linezolid (12 mg kg^{-1}), Dipi-van (12 mg kg^{-1}), or saline. 72 h after the initial treatment, the antibacterial activity was determined by measuring the bacterial titer in the infected kidneys. Compared to vancomycin, Dipi-van and linezolid reduced the bacterial titer in the infected kidneys more effectively. Linezolid achieved a CFU reduction of 4 $\log_{10}$ compared to the vehicle-treated control (saline), whereas Dipi-van led to a CFU reduction of approximately 5 $\log_{10}$ (Figure 3B).

In summary, a simple rational strategy has been presented to combat the acquired resistance of Gram-positive bacteria towards glycopeptide antibiotics. The new compound, Dipi-van, was approximately two orders of magnitude more active against vancomycin-resistant bacteria than vancomycin. Furthermore, Dipi-van showed potent in vivo activity against VRE compared to linezolid and vancomycin and displayed no significant toxicity. Our results demonstrate the high therapeutic potential of Dipi-van to address the clinical challenge of vancomycin-resistant bacterial infections.

Acknowledgements

We thank Prof. C. N. R. Rao, FRS (JNCASR) for his constant support and encouragement. S.S. is grateful to the Sheikh Saqr laboratory at JNCASR for a post-doctoral fellowship. We thank Dr. R. G. Prakash (in-house animal facility) for his help with the in vivo studies.

Keywords: antibiotics · bacterial resistance · drug design · multidrug-resistant bacteria · vancomycin

How to cite: *Angew. Chem. Int. Ed.* **2016**, *55*, 7836–7840
Angew. Chem. **2016**, *128*, 7967–7971

[1] a) D. P. Levine, *Clin. Infect. Dis.* **2006**, *42*, S5–S12; b) M. S. Butler, K. A. Hansford, M. A. Blaskovich, R. Halai, M. A. Cooper, *J. Antibiot.* **2014**, *67*, 631–644; c) S. Y. C. Tong, J. S. Davis, E. Eichenberger, T. L. Holland, V. G. Fowler, Jr., *Clin. Microbiol. Rev.* **2015**, *28*, 603–661; d) D. Kahne, C. Leimkuhler, W. Lu, C. T. Walsh, *Chem. Rev.* **2005**, *105*, 425–448.
[2] a) K. Hiramatsu, *Lancet Infect. Dis.* **2001**, *1*, 147–155; b) L. M. Weigel, D. B. Clewell, S. R. Gill, N. C. Clark, L. K. McDougal, S. E. Flannagan, J. F. Kolonay, J. Shetty, G. E. Killgore, F. C. Tenover, *Science* **2003**, *302*, 1569–1571.
[3] G. Taubes, *Science* **2008**, *321*, 356–361.
[4] a) R. P. Wenzel, M. B. Edmond, *N. Engl. J. Med.* **2000**, *343*, 1961–1963; b) S. B. Levy, B. Marshall, *Nat. Med.* **2004**, *10*, S122–S129; c) M. A. Fischbach, C. T. Walsh, *Science* **2009**, *325*, 1089–1093.

[5] a) B. Gu, T. Kelesidis, S. Tsiodras, J. Hindler, R. M. Humphires, *J. Antimicrob. Chemother.* **2013**, *68*, 4 – 11; b) U. Bertsche et al., *PLoS One* **2013**, *8*, e67398.

[6] a) K. Lewis, *Nat. Rev. Drug Discovery* **2013**, *12*, 371 – 387; b) K. Bush et al., *Nat. Rev. Microbiol.* **2011**, *9*, 894 – 896; c) E. D. Brown, G. D. Wright, *Nature* **2016**, *529*, 336 – 343.

[7] a) K. M. G. O'Connell, J. T. Hodgkinson, H. F. Sore, M. Welch, G. P. C. Salmond, D. R. Spring, *Angew. Chem. Int. Ed.* **2013**, *52*, 10706 – 10733; *Angew. Chem.* **2013**, *125*, 10904 – 10932; b) G. L. Thomas et al., *Angew. Chem. Int. Ed.* **2008**, *47*, 2808 – 2812; *Angew. Chem.* **2008**, *120*, 2850 – 2854; c) G. Guchhait, A. Altieri, B. Gorityala, X. Yang, B. Findlay, G. G. Zhanel, N. Mookherjee, F. Schweizer, *Angew. Chem. Int. Ed.* **2015**, *54*, 6278 – 6282; *Angew. Chem.* **2015**, *127*, 6376 – 6380; d) N. Barraud et al., *Angew. Chem. Int. Ed.* **2012**, *51*, 9057 – 9060; *Angew. Chem.* **2012**, *124*, 9191 – 9194.

[8] a) C. Ghosh, G. B. Manjunath, P. Akkapeddi, V. Yarlagadda, J. Hoque, D. S. Uppu, M. M. Konai, J. Haldar, *J. Med. Chem.* **2014**, *57*, 1428 – 1436; b) M. M. Konai, C. Ghosh, V. Yarlagadda, J. Haldar, *J. Med. Chem.* **2014**, *57*, 9409 – 9423; c) D. S. S. M. Uppu, P. Akkapeddi, G. B. Manjunath, V. Yarlagadda, J. Hoque, J. Haldar, *Chem. Commun.* **2013**, *49*, 9389 – 9391; d) H. Wu, Y. Niu, S. Padhee, R. E. Wang, Y. Li, Q. Qiao, G. Bai, C. Cao, J. Cai, *Chem. Sci.* **2012**, *3*, 2570 – 2575; e) M. M. Konai, J. Haldar, *ACS Infect. Dis.* **2015**, *1*, 469 – 478; f) C. Ghosh, G. B. Manjunath, M. M. Konai, D. S. S. M. Uppu, J. Hoque, K. Paramanandham, B. R. Shome, J. Haldar, *ACS Infect. Dis.* **2016**, *2*, 111 – 122.

[9] a) A. Makovitzki, D. Avrahami, Y. Shai, *Proc. Natl. Acad. Sci. USA* **2006**, *103*, 15997 – 16002; b) S. Choi, A. Isaacs, D. Clements, D. Liu, H. Kim, R. W. Scott, J. D. Winkler, W. F. Degrado, *Proc. Natl. Acad. Sci. USA* **2009**, *106*, 6968 – 6973; c) B. P. Mowery, S. E. Lee, D. A. Kissounko, R. F. Epand, B. Weisblum, S. S. Stahl, S. H. Gellman, *J. Am. Chem. Soc.* **2007**, *129*, 15474 – 15476; d) M. Wenzel et al., *Proc. Natl. Acad. Sci. USA* **2014**, *111*, E1409 – E1418; e) R. Liu et al., *J. Am. Chem. Soc.* **2014**, *136*, 4410 – 4418; f) P. Chairatana, T. Zheng, E. M. Nolan, *Chem. Sci.* **2015**, *6*, 4458 – 4471.

[10] a) J. R. Morones-Ramirez, J. A. Winkler, C. S. Spina, J. J. Collins, *Sci. Transl. Med.* **2013**, *5*, 190ra81; b) T. Zheng, E. Nolan, *J. Am. Chem. Soc.* **2014**, *136*, 9677 – 9691; c) P. I. O'Daniel et al., *J. Am. Chem. Soc.* **2014**, *136*, 3664 – 3672; d) Y. Li, G. Liu, X. Wang, J. Hu, S. Liu, *Angew. Chem. Int. Ed.* **2016**, *55*, 1760 – 1764; *Angew. Chem.* **2016**, *128*, 1792 – 1796; e) B. K. Gorityala, G. Guchhait, D. M. Fernando, S. Deo, S. A. McKenna, G. G. Zhanel, A. Kumar, F. Schweizer, *Angew. Chem. Int. Ed.* **2016**, *55*, 555 – 559; *Angew. Chem.* **2016**, *128*, 565 – 569.

[11] a) L. L. Ling et al., *Nature* **2015**, *517*, 455 – 459; b) B. P. Conlon, E. S. Nakayasu, L. E. Fleck, M. D. LaFleur, V. M. Isabella, K. Coleman, S. N. Leonard, R. D. Smith, J. N. Adkins, K. Lewis, *Nature* **2013**, *503*, 365 – 370; c) M. N. Thaker, W. Wang, P. Spanogiannopoulos, N. Waglechner, A. M. King, R. Medina, G. D. Wright, *Nat. Biotechnol.* **2013**, *31*, 922 – 927.

[12] a) X. Fu, C. Albermann, J. Jiang, J. Liao, C. Zhang, J. S. Thorson, *Nat. Biotechnol.* **2003**, *21*, 1467 – 1469; b) L. Chen, D. Walker, B. Sun, Y. Hu, S. Walker, D. Kahne, *Proc. Natl. Acad. Sci. USA* **2003**, *100*, 5658 – 5663; c) P. A. Ashford, S. P. Bew, *Chem. Soc. Rev.* **2012**, *41*, 957 – 978; d) S. Yoganathan, S. J. Miller, *J. Med. Chem.* **2015**, *58*, 2367 – 2377; e) Y. Nakama, O. Yoshida, M. Yoda, K. Araki, Y. Sawada, J. Nakamura, S. Xu, K. Miura, H. Maki, H. Arimoto, *J. Med. Chem.* **2010**, *53*, 2528 – 2533.

[13] a) C. T. Walsh, S. L. Fisher, I. S. Park, M. Prahalad, Z. Wu, *Chem. Biol.* **1996**, *3*, 21 – 28; b) C. C. McComas, B. M. Crowley, D. L. Boger, *J. Am. Chem. Soc.* **2003**, *125*, 9314 – 9315; c) J. Pootoolal, J. Neu, G. D. Wright, *Annu. Rev. Pharmacol. Toxicol.* **2002**, *42*, 381 – 408.

[14] a) J. Rao, J. Lahiri, L. Isaacs, R. M. Weiss, G. M. Whitesides, *Science* **1998**, *280*, 708 – 711; b) J. H. Griffin et al., *J. Am. Chem. Soc.* **2003**, *125*, 6517 – 6531; c) K. C. Nicolaou, R. Hughes, S. Y. Cho, N. Winssinger, C. Smethurst, H. Labischinski, R. Endermann, *Angew. Chem. Int. Ed.* **2000**, *39*, 3823 – 3828; *Angew. Chem.* **2000**, *112*, 3981 – 3986; d) R. C. James, J. G. Pierce, A. Okano, J. Xie, D. L. Boger, *ACS Chem. Biol.* **2012**, *7*, 797 – 804; e) J. Xie, J. G. Pierce, R. C. James, A. Okano, D. L. Boger, *J. Am. Chem. Soc.* **2011**, *133*, 13946 – 13949; f) J. Xie, A. Okano, J. G. Pierce, R. C. James, S. Stamm, C. M. Crane, D. L. Boger, *J. Am. Chem. Soc.* **2012**, *134*, 1284 – 1297; g) V. Yarlagadda, M. M. Konai, G. B. Manjunath, C. Ghosh, J. Haldar, *J. Antibiot.* **2015**, *68*, 302 – 312; h) V. Yarlagadda, M. M. Konai, K. Paramanandham, B. R. Shome, J. Haldar, *Int. J. Antimicrob. Agents* **2015**, *46*, 446 – 450; i) V. Yarlagadda, P. Sarkar, G. B. Manjunath, J. Haldar, *Bioorg. Med. Chem. Lett.* **2015**, *25*, 5477 – 5480.

[15] a) F. Van Bambeke, M. P. Mingeot-Leclercq, M. J. Struelens, P. M. Tulkens, *Trends Pharmacol. Sci.* **2008**, *29*, 124 – 134; b) D. L. Higgins et al., *Antimicrob. Agents Chemother.* **2005**, *49*, 1127 – 1134; c) O. Domenech, G. Francius, P. M. Tulkens, F. Van Bambeke, Y. Dufrene, M. P. Mingeot-Leclercq, *Biochim. Biophys. Acta Biomembr.* **2009**, *1788*, 1832 – 1840; d) V. Yarlagadda, P. Akkapeddi, G. B. Manjunath, J. Haldar, *J. Med. Chem.* **2014**, *57*, 4558 – 4568; e) V. Yarlagadda et al., *Int. J. Antimicrob. Agents* **2015**, *45*, 627 – 634; f) V. Yarlagadda, S. Samaddar, K. Paramanandham, B. R. Shome, J. Haldar, *Angew. Chem. Int. Ed.* **2015**, *54*, 13644 – 13649; *Angew. Chem.* **2015**, *127*, 13848 – 13853; g) V. Yarlagadda, G. B. Manjunath, P. Sarkar, P. Akkapeddi, K. Paramanandham, B. R. Shome, R. Ravikumar, J. Haldar, *ACS Infect. Dis.* **2016**, *2*, 132 – 139; h) V. Yarlagadda, S. Samaddar, J. Haldar, *J. Global Antimicrob. Resist.* **2016**, DOI: 10.1016/j.jgar.2015.12.007.

[16] a) E. Breukink, B. de Kruijff, *Nat. Rev. Drug Discovery* **2006**, *5*, 321 – 323; b) B. de Kruijff, V. van Dam, E. Breukink, *Prostaglandins, Leukotrienes Essent. Fatty Acids* **2008**, *79*, 117 – 121.

[17] a) H. T. Ngo, X. Liu, K. A. Jolliffe, *Chem. Soc. Rev.* **2012**, *41*, 4928 – 4965; b) K. J. Clear, K. M. Harmatys, D. R. Rice, W. R. Wolter, M. A. Suckow, Y. Wang, M. Rusckowski, B. D. Smith, *Bioconjugate Chem.* **2016**, *27*, 363 – 375.

[18] a) C. A. McDevitt, A. D. Ogunniyi, E. Valkov, M. C. Lawrence, B. Kobe, A. G. McEwan, J. C. Paton, *PLoS Pathog.* **2011**, *7*, e1002357; b) C. E. Outten, T. V. O'Halloran, *Science* **2001**, *292*, 2488 – 2492.

[19] T. Schneider et al., *Science* **2010**, *328*, 1168 – 1172

Received: February 15, 2016
Revised: March 7, 2016
Published online: March 24, 2016

